Level structure of 99Nb

Lhersonneau, G.; Suhonen, J.; Dendooven, P.; Honkanen, A.; Huhta, M.; Jones, P.; Julin, R.; Juutinen, S.; Oinonen, M.; Penttila, H.; ...

Source / Izvornik: **Physical Review C - Nuclear Physics, 1998, 57, 2974 - 2990**

Journal article, Published version
Rad u časopisu, Objavljena verzija rada (izdavačev PDF)

https://doi.org/10.1103/PhysRevC.57.2974

Permanent link / Trajna poveznica: https://urn.nsk.hr/urn:nbn:hr:217:984591

Rights / Prava: In copyright / Zaštićeno autorskim pravom.

Download date / Datum preuzimanja: **2025-03-27**

Repository / Repozitorij:

Repository of the Faculty of Science - University of Zagreb

Level structure of ^{99}Nb

G. Lhersonneau, J. Suhonen, P. Dendooven, A. Honkanen, M. Huhta, P. Jones, R. Julin, S. Juutinen, M. Oinonen, H. Penttilä, J. R. Persson,* K. Peräjärvi, A. Savelius, J. C. Wang, and J. Äystö
Department of Physics, University of Jyväskylä, P.O. Box 35, FIN-40351, Jyväskylä, Finland

S. Brant, V. Paar, and D. Vretenar
Department of Physics, Faculty of Science, University of Zagreb, 10000 Zagreb, Croatia
(Received 5 February 1998)

The β decay of ^{97}Sr to ^{97}Y has been investigated using ion-guide on-line mass separation and a 10 Ge-detector array to record γ-γ coincidences to a detection limit well below that of former studies. Similarities are found in the β-decay patterns of ^{99}Zr and of its isotone ^{97}Sr and also in the γ-ray decay rates and branchings of the corresponding levels in their respective daughters ^{99}Nb and ^{97}Y. This indicates a persisting influence of the $d_{5/2}$ neutron shell closure for ^{99}Nb. The level structure of ^{99}Nb and the β-feeding pattern are discussed in the frame of the interacting boson-fermion plus broken pair model and the microscopic quasiparticle phonon model. [S0556-2813(98)06106-8]

PACS number(s): 27.60.+j, 21.10.Tg, 23.20.Lv

I. INTRODUCTION

Neutron-rich nuclei near $^{96}_{40}Zr_{56}$ have been investigated in numerous studies motivated by the strong shell closure associated with the neutron $d_{5/2}$ subshell filling when protons occupy the natural parity states below the $g_{9/2}$ orbital [1]. Nuclei with a few valence particles with respect to ^{96}Zr are especially interesting owing to the rapidly changing level structure with increasing nucleon number. With the addition of only four neutrons, the ground states of the neighboring $N=60$ isotones become strongly deformed [2]. Deformations are as large as $\beta \simeq 0.40$ for $^{98}_{38}$Sr [3] and $^{99}_{39}$Y [4], while they slightly decrease with increasing Z [5,6,5–8]. Shape coexistence has been reported for the $N=59$ isotones ^{97}Sr [9–11] and ^{98}Y [12–14], both of which have spherical ground states and deformed states at about 0.5 MeV excitation energy. However, for ^{99}Zr a clear indication for an excited deformed band structure is still lacking [15–18]. The lowest-lying levels in ^{97}Sr and ^{99}Zr present similarities with the levels in the $N=57$ isotones ^{95}Sr [19] and ^{97}Zr [20], whereas in their ^{99}Mo [21] and ^{101}Mo [22] neighbors one observes an evolution of the level structure versus neutron number. This different behavior versus proton number is related to the vanishing of the $d_{5/2}$ neutron shell closure we have recently discussed for ^{99}Mo [21]. The $N=58$ isotones with $Z \leqslant 40$ display clear fingerprints of shell closure effects. The 2_1^+ states in even-even Sr isotopes have almost constant energies at $\sim$0.8 MeV from ^{90}Sr to ^{96}Sr. Their low collectivity has been established by lifetime measurements [23]. High-spin levels in the odd-proton nucleus ^{97}Y have been observed via isomeric decay of an $I^\pi = 27/2^-$ isomer [24]. The high-spin level structure of ^{97}Y has been calculated in the frame of the interacting boson-fermion model (IBFM) [25] and, very recently, by its extended version including a broken neutron pair [26]. The ^{98}Zr nucleus has a high-lying 2_1^+ state at 1223 keV. In contrast, the 2_1^+ energy in ^{100}Mo is only 536 keV.

Thus, there is a dramatic change of the level structure of $N \leqslant 59$ spherical nuclei associated with the closure of the $g_{7/2}$-$d_{5/2}$ neutron gap when proton pairs start to occupy the $g_{9/2}$ shell. With its proton number of $Z=41$, the nucleus ^{99}Nb is situated at the transition between the region where the $N=56$ shell closure is active ($Z \leqslant 40$) and the region of the open shell ($Z \geqslant 42$). In this context, a detailed study of ^{99}Nb levels should provide an insight into the influence of a single $g_{9/2}$ proton on the $d_{5/2}$ neutron-shell closure. Especially appealing is the comparison of levels in the $N=58$ isotones ^{97}Y and ^{99}Nb. These are populated by β decay of ^{97}Sr and ^{99}Zr which have a very similar low-lying level structure [9,15]. Accordingly, levels of the same character might be selected by β decay into ^{97}Y and ^{99}Nb and this should provide a means to follow their evolution when the proton number crosses $Z=40$.

The low-spin levels in ^{97}Y have been studied by β decay of $I^\pi = 1/2^+$ ^{97}Sr by Pfeiffer *et al.* [27]. Level-lifetime measurements were subsequently performed by the TRISTAN group [10] according to which several levels were interpreted as core + particle configurations. For a better comparison of the levels in the isotones ^{97}Y and ^{99}Nb we have reinvestigated the ^{97}Y level scheme using γ-γ coincidence data recorded during former experiments [20,24].

The levels in ^{99}Nb have been studied by the decay of $I^\pi = 1/2^+$ ^{99}Zr, including lifetime measurements [28], and several transfer reactions, compiled in the Nuclear Data Sheets [29]. An extended decay scheme, compared to that published in Ref. [29], was presented by Pfeiffer *et al.* [30]. The so far reported transitions have intensities of about 1% per decay. It has been shown that experiments at the IGISOL facility, see, e.g., Refs. [20,21], allow the detection of transitions with still lower branchings for most of the neutron-rich isotopes in this region. The observation of new weak γ-ray branchings, combined with absolute transition probabilities should provide a basis for firm spin and parity as-

*Present address: Cyclotron Laboratory, RIKEN, Wako-Shi, Saitama 351-01, Japan.

 © 1998 The American Physical Society

signments. In addition, the question of whether a $27/2^-$ three quasiparticle state could form an isomer, similar to the one in ^{97}Y, is still open [21]. If this configuration has a half-life of about 1 ms or longer, high-spin states in ^{99}Nb could be observed using on-line mass separation with the ion-guide technique.

Finally, shape coexistence has been proposed for ^{98}Zr, the isotone of ^{99}Nb, based on the large $\rho^2(0_3^+ \rightarrow 0_2^+)$ value of 0.075 [15]. However, a strongly deformed band built on this 0_3^+ state at 1436 keV has not been observed in a recent prompt-fission study [18]. To our knowledge, there have not been reports of shape coexistence in neutron-rich Nb isotopes. Unfortunately, it is unlikely that a band structure will be observed after the β decay of the $1/2^+$ ground state of ^{99}Zr.

II. EXPERIMENTS

The main experiment was devoted to the decay of ^{99}Zr to ^{99}Nb, which is described below. For the purpose of systematics some details of the decay scheme of ^{97}Sr to ^{97}Y were to be studied in greater detail. The data have been obtained from previous experiments [20,24] which we do not present here.

A. Production of ^{99}Zr and detector setup

The parent nucleus of ^{99}Nb, ^{99}Zr, was produced by fission of a natural U target induced by 25 MeV protons delivered as a 50 MeV H_2^+ beam, thus doubling the particle intensity. The beam intensity was typically 10 p μA. The $A=99$ isobars were separated on-line using the IGISOL technique [31–33]. The mass separated beams were collected on a movable tape viewed by various detectors for β particles and γ rays. The ^{99}Y ($T_{1/2}=1.5$ s) and ^{99}Zr ($T_{1/2}=2.1$ s) activities [34] are produced with comparable independent yields of about 5×10^3 ions/s. Hence, the cumulative yield of ^{99}Zr, which includes the contribution of the β decay of ^{99}Y, is roughly twice that of ^{99}Y. As a consequence of the similar half-lives of the ^{99}Y and ^{99}Zr activities, their discrimination requires acquisition cycles with a long decay period. This reduces the duty cycle and the counting statistics. Therefore, two sets of experiments were performed, following the procedures described in recent papers [20,21]. First, coincidences were recorded with a 10 Ge-detector array (DORIS), a more compact version of the 12 Ge-detector TARDIS array described in [24], providing an improvement of a factor of 1.9 for twofold events. One of the detectors was a planar Ge detector for low-energy radiation. In order to collect the largest number of events, the beam was continuously implanted in the center of the array and the tape was moved at various time intervals in order to enhance one or the other activity. The coincidences were recorded with the EUROGAM data acquisition system [35]. Secondly, a setup consisting of two thin plastic scintillators for β particles, the low-energy Ge detector and a coaxial detector of 23% efficiency covering a range of energies up to 3.6 MeV, was used. The goal of this experiment was to record β-γ-time coincidences and to identify the activities on the basis of growth and decay curves of the γ rays. For this purpose, the separator beam was pulsed and the collecting tape was moved after each beam on/off sequence. Pure singles, e.g., non-β-gated spectra, of the low-energy detector were also recorded in order to allow the observation of occasional isomeric transitions. The data were recorded with the VENLA data acquisition system [36] designed at the Accelerator Laboratory in Jyväskylä. A time to digital converter (TDC) marking the time of occurence of events with respect to the beginning of the separator cycle was written as an additional list-mode parameter.

B. Analysis

The coincidence data taken with the DORIS array were first sorted off-line to construct γ-γ and x-γ matrices. Higher-fold events were also investigated, which could have given an indication of a cascade of high multiplicity following the decay of the high-spin isomer postulated to exist in ^{99}Nb. The additional experiments yielded further TDC-γ and TAC-γ matrices (where the time-to-amplitude converter recorded the time between β and γ rays for the determination of level lifetimes). For both experiments, energy and efficiency calibrations were performed internally, using data compiled in [29] and our results on the decay of ^{99}Nb to ^{99}Mo [21]. Since the ^{99}Nb level scheme contains several strong low-energy transitions, we describe in some detail the determination of conversion coefficients which are obtained from coincidence data. Intensity balance considerations for transitions observed in gates set on γ rays placed above the the converted transition yield the total conversion coefficient α. They are reliable since they use medium- or high-energy γ-γ data which can be calibrated accurately. Unfortunately, the measured quantity is $1+\alpha$, which is not very sensitive if α is small. A more direct method, giving α_K, is based on the fluorescence produced by the converted transition. It, however, requires an accurate efficiency calibration of the gated spectra at the low-energies of the K-x rays. This is rather difficult due to the scarcity of internal references. Nevertheless, the K-x rays due to the conversion of some transitions of known multipolarity could be observed under sufficiently clean conditions in various gates set on the Ge detectors. These were the transitions of 98 keV ($E2$, ^{99}Mo), 130 keV ($E2$, ^{99}Zr), and 36 keV ($E1$, ^{98}Y [12]). The higher-energy part of the on-line efficiency curve of the x-ray detector was determined by comparison with off-line calibrations made with ^{133}Ba, ^{152}Eu, and ^{241}Am standards [34]. Owing to the distribution of the Ge detectors over the whole solid angle, angular-correlation effects were not likely to play a major role with respect to the rather large statistical uncertainties. These have not been taken into account. In addition, these measurements yielded a value of $\alpha_K=0.13(3)$ for the 122 keV transition in ^{99}Zr, confirming its $M1$ multipolarity.

III. RESULTS

A. Decay scheme of ^{99}Zr to ^{99}Nb

The decay scheme is based mostly on coincidence data using the previously reported transitions [29] as a starting point. As a matter of fact, the detection limit for lines in the singles spectra was poorer than in the coincidence data by about one order of magnitude. Thus, weakly populated $I=(1/2,3/2)$ levels which only decay to the $1/2^-$ isomer remain unidentified if the relative transition intensity is below

1%. This, however, should not modify the conclusions about the presence of very strongly β-fed levels near 1 MeV.

The decay scheme now includes 33 transitions placed between 13 levels. Although transitions weaker than 0.1 relative intensity units have been observed, there are only five new levels with respect to the decay data compiled in Ref. [29]. Some of these have already been reported by Pfeiffer *et al.* [30] in their decay work or in the transfer-reaction study by Flynn *et al.* [37]. Transitions and their coincidence relationships are shown in Table I. Several of the listed transitions cannot be placed unambiguously, although there is fair evidence that they belong to the level scheme of ^{99}Nb. The coincidence pair 88.8–561.4 keV is assigned to ^{99}Nb by the K-x rays originating from the conversion of the 89 keV transition, see Table II. There are no other coincidence relationships involving these lines but their sum of 650.2 keV compares well with the energy difference of the 1015.4 keV level and the isomer at 365.4 keV, so that this cascade probably fits between these levels. The 363.0 and 379.2 keV transitions have very weak coincidences, but which seem to form a consistent set according to which they should be placed below the 387.5 keV level. A transition of 24.3 keV observed randomly in various gates could correspond to the 387.5–363.0 keV energy difference. Nevertheless, we regard the existence of levels at 363 and 379 keV as speculative. Another weak coincidence pair is formed by the lines at 444.5 and 600.4 keV, the sum of which may fit from the 1044.5 keV level to the ground state. However, there are no other data to assign these transitions to ^{99}Nb. A level at 1005.7 keV is uncertain, since based on two sums involving the weak 46.1 keV (a possible Ge-x-ray escape of the strong 56 keV line) and 536.7 keV γ rays (which might be a residual of the strong 536.1 keV line in ^{99}Zr). Finally, the weak peaks at 930.8 and 1015.7 keV seen in the single spectra are interpreted as due to coincidence summing of the 461.9 and 546.1 keV transitions, respectively, with the 469.2 keV transition placed below them.

The results confirm the previously adopted level scheme [29], except for the intensity of the 28.4 keV transition to the 930.8 keV level. This fact turns out to be of importance, since it allows a more consistent interpretation of the spin and parity assignments of the ^{99}Nb levels. The 28 keV transition was reported with an intensity $I_\gamma \simeq 3$ relative intensity units. Taking electron conversion into account, the intensity balance of the 930.8 keV level could be achieved only in the absence of direct β feeding. In the present experiment, however, a much lower total intensity *including conversion* of $I_t(28) = 2.4(4)$ is deduced by comparing the peak area of the 56 keV transition in the 461 and 594 keV gates as shown in Fig. 1. The intensity balance now requires allowed β feeding into the 959 keV level and this implies $I^\pi(931) = (1/2,3/2)^+$ in contrast to the former $5/2^+$ assignment.

Conversion coefficients are shown in Table II. The multipolarities formerly assigned to the 28.4, 55.9, and 81.8 keV transitions, mostly on the basis of balancing the level feedings [29], are confirmed. An $E2$ admixture, 10(8)% using both K and total conversion coefficients, could be present in the 82 keV transition. The conversion coefficient for the new 114.2 keV transition is suggestive of a pure $E2$ multipolarity. This is, however, not consistent with its lifetime limit [28], so that it has to be rather a $M1$ transition with an $E2$ component.

B. Spin and parity assignments of ^{99}Nb levels

The decay scheme of ^{99}Zr to ^{99}Nb is shown in Fig. 2 and the properties of the levels are summarized in Table III. The neighbors of ^{99}Nb are ^{98}Zr and ^{100}Mo which do not exhibit rotational structure at low energy. For this reason, strongly enhanced $E2$ transitions are not expected to occur between the low-lying levels of ^{99}Nb. This assumption is the key for the following spin and parity assignments.

The allowed β branches for the decay of $I^\pi = 1/2^+$ ^{99}Zr to three levels near 1 MeV provide a starting point for the analysis. The strongest cascade is formed by the 546.1 and 469.2 keV transitions. The logft value of 4.1 for the level at 1015.4 keV implies $I^\pi = (1/2,3/2)^+$ and, since the ground state has $I^\pi = 9/2^+$, at least one of the 546 or 469 keV transitions must be of pure quadrupole character. The lifetime limits of Ref. [28] for both the 1015 and 469 keV levels obviously exclude $M2$ multipolarities, which results in $I^\pi = (5/2,7/2)^+$ for the intermediate 469 keV level. The enhancement factors for the 469 and 546 keV transitions, if $E2$, are 4.8 and >70, respectively. Therefore, we conclude that the 546 keV transition is not an $E2$ but a $M1$ and the 469 keV transition is the $E2$. The spin and parity of the 469 keV and 1015 keV levels are thus $I^\pi = 5/2^+$ and $3/2^+$, respectively.

The 387.5 keV level is fed from the 469 keV level via the 81.8 keV transition of $M1$ character (see Table II), which restricts its spin and parity to $I^\pi = (5/2,7/2)^+$. From the lifetime of the 387 keV level [28] an enhancement of 137 would result for the 387 keV ground-state transition if it were an $E2$. Therefore, we adopt the $M1$ alternative and assign $I^\pi(387) = 7/2^+$. Then, the 628 keV transition from the $3/2^+$ level at 1015 keV must be another $E2$. The transition rate limit of >1.6 deduced from the partial lifetime, is indeed low enough to leave room for a moderately enhanced transition. These assignments were also made by Ohm [28], in contrast to the very first interpretations [39,40].

As a new result, the 931.0 keV level is directly fed in β decay. The logft value of 4.9 implies $I^\pi(931) = (1/2,3/2)^+$, instead of $I^\pi = 5/2^+$ [40]. We can use the same kind of argument as above to show that the 462 keV transition to the 469 keV $5/2^+$ level would have had an enhancement >89 if an $E2$. Accordingly, we choose the $M1$ alternative and assign $I^\pi(931) = 3/2^+$. Both $3/2^+$ levels at 931 and 1015 keV have a similar γ-ray branching pattern. Here also, an $E2$ transition to the 387 keV level exists. The decay rate for this 543.6 keV transition is >2.4 single-particle units, which is an acceptable limit.

The 959.4 keV level is the last of the levels strongly fed by a direct β-decay branch (logft=4.4), which again allows $I^\pi = (1/2,3/2)^+$ as the only possible choices. Constrained by the dipole character of the 28 keV transition to the 931 keV level, formerly a $5/2^+$ state, Ohm assigned $I^\pi(959) = 3/2^+$. However, the γ-decay pattern of the 959 keV level is very different from those of the 931 and 1015 keV levels. The largest branching goes to the $1/2^-$ isomeric level at 365 keV. The decay to the $5/2^+$ level at 469 keV is weak and a transition to the 387 keV $7/2^+$ state could not be detected. This

TABLE I. List of γ rays in the decay of ^{99}Zr to ^{99}Nb. Intensities are calculated from coincidence data and in most cases also from singles unless specified. For absolute decay intensity multiply I_γ by 0.562×10^{-2}.

Energy (keV)		Intensity	Placed from	Placed to	Coincidences
28.4 (1)		0.39 (11)	959	931	56, 82, (387), 462, 469
46.1 (3)	[a]	0.12 (6)	(1005	959)	(594)
55.9 (1)		3.9 (7)	1015	959	K-x$_{Nb}$, 28, 82, 179, (387), 415, 462, 469, (490), 594
74.3 (4)	[b]	0.02 (1)	544	469	(415), (469)
81.8 (1)		5.8 (8)	469	387	K-x$_{Nb}$, (28), (56), (113), (363), (379), 387, 462, 490, 546, 575
84.4 (2)	[c]	0.16 (3)	1015	931	462, 469
86.7 (3)	[b]	0.07 (2)	631	544	179, (385)
88.8 (2)	[a]	0.09 (2)			561
113.4 (4)	[b]	0.06 (2)	1044	931	(462), (469)
114.2 (2)	[c]	0.31 (7)	931	817	(K-x$_{Nb}$), (348), 387, 429, 817
165.6 (3)	[b]	0.01 (1)	931	765	(221)
175.2 (5)	[a]	0.09 (3)	(644	469)	(469)
178.9 (2)		10.2 (16)	544	365	K-x$_{Nb}$, 56, 87, 221, 250, (385), 386, 415, 471, 500
198.0 (5)	[c]	0.06 (2)	1015	817	(429), (817)
220.9 (2)	[b]	0.08 (2)	765	544	(166), 179, 250
250.4 (3)	[b]	0.04 (1)	1015	765	(179), (221)
347.5 (3)	[b]	0.08 (2)	817	469	(114), (469)
363.0 (5)	[a]	0.06 (3)			(82), (546), (628)
379.2 (5)	[a]	0.10 (3)			(82), (546), (628)
384.8 (3)	[b]	0.06 (2)	1015	631	(87), (179)
386.5 (3)	[b]	0.11 (3)	931	544	179
387.5 (2)	[d]	14.8 (23)	387	0	K-x$_{Nb}$, 82, 114, 429, 462, 490, 543, 546, (575), 628
415.1 (2)		8.3 (7)	959	544	K-x$_{Nb}$, 56, (74), 179
429.3 (3)	[c]	0.38 (8)	817	387	114, 198, 387
444.5 (4)	[a]	0.06 (2)			
461.9 (2)		20.1 (22)	931	469	K-x$_{Nb}$, 28, 56, 82, 84, (113), 387, 469, (1043)
469.2 (2)		100	469	0	K-x$_{Nb}$, 28, 56, (84), (113), (175), (198), (348), 462, 490, (536), 546, 575, 959, (1043), (1321)
471.1 (3)	[b]	0.12 (4)	1015	544	(179)
490.2 (3)		0.98 (16)	959	469	(K-x$_{Nb}$), 56, 82, 387, 469
499.9 (3)	[b]	0.06 (2)	1044	544	(179)
536.7 (3)	[a]	1.5 (4)	(1005	469)	(81), (387), (469)
543.6 (4)	[c]	1.26 (18)	931	387	(K-x$_{Nb}$), (28), (387)
546.1 (2)		84.9 (64)	1015	469	K-x$_{Nb}$, 82, (363), 387, 469, 959, (1321)
561.4 (3)	[a]	0.19 (6)			(K-x$_{Nb}$), 89
575.4 (3)	[b]	1.63 (42)	1044	469	82, 387, 469
594.1 (2)		46.9 (54)	959	365	K-x$_{Nb}$, 56
600.4 (4)	[a]	0.06 (2)			(444)
628.0 (2)		4.0 (6)	1015	387	387
650.0 (2)	[d]	4.1 (8)	1015	365	
816.7 (3)	[c]	0.12 (4)	817	0	114, (198)
930.8 (4)	[e]	0.9 (3)			
959.4 (3)		0.61 (12)	1975	1015	(56), 469, 546
1015.7 (4)	[e]	2.6 (7)			(K-x$_{Nb}$)
1043.4 (4)	[c]	0.18 (4)	1975	931	(462), (469)
1321.0 (3)	[c]	0.24 (6)	2336	1015	(469), (546)

[a]Possible transition of uncertain placement in ^{99}Nb.

[b]New transition from this work.

[c]Reported by Pfeiffer *et al.* [30].

[d]Intensity was determined from singles only.

[e]Peak due to coincidence summing.

TABLE II. Conversion coefficients obtained from γ-γ and x-γ coincidences. Theoretical values are obtained from [38].

Energy (keV)	Measured		Theoretical $E1$	Theoretical $M1$	Theoretical $E2$	Adopted
28.4	7.2(26)	[a]	3.7	7.6	46	$M1$
	6.1(20)	[b]	4.3	8.7	108	
55.9	1.12(25)	[c]	0.57	1.05	6.7	$M1$
81.8	0.53(12)	[d]	0.19	0.35	1.9	$M1$
	0.50(24)	[e]	0.22	0.40	2.4	
88.8	1.13(45)	[f]	0.15	0.28	1.4	$E2$, ($M1$)
114.2	0.57(26)	[g]	0.072	0.14	0.59	$M1+E2$
178.9	0.065(27)	[h]	0.020	0.041	0.119	$M1$

[a] α_K from gate on 462 keV, corrected for contributions of 56 and 82 keV γ rays to $K\alpha$-x peak.
[b] α from comparison of $I_\gamma(594)$ and $I_\gamma(462)$ in gate on 56 keV yielding $I_t(28)=2.50(65)$ and 2.33(45) from x-γ and γ-γ data, respectively.
[c] α_K from gate on 594 keV.
[d] α_K from gate on 546 keV, corrected for contribution of 469 keV γ ray to $K\alpha$-x peak.
[e] α from comparison of $I_\gamma(82)$ and $I_\gamma(387)$ in gates 462 and 546 keV.
[f] α_K from gate on 561 keV, this transition is unplaced.
[g] α_K from gate on 429 keV, corrected for contributions of 28 keV and K_β(Y) due to 52–428–119 keV cascade in ^{98}Y [12] to the $K\alpha$-x peak. Pure $E2$ excluded by the lifetime.
[h] α_K from gate on 415 keV, corrected for contribution of the 56 keV to the $K\alpha$-x peak.

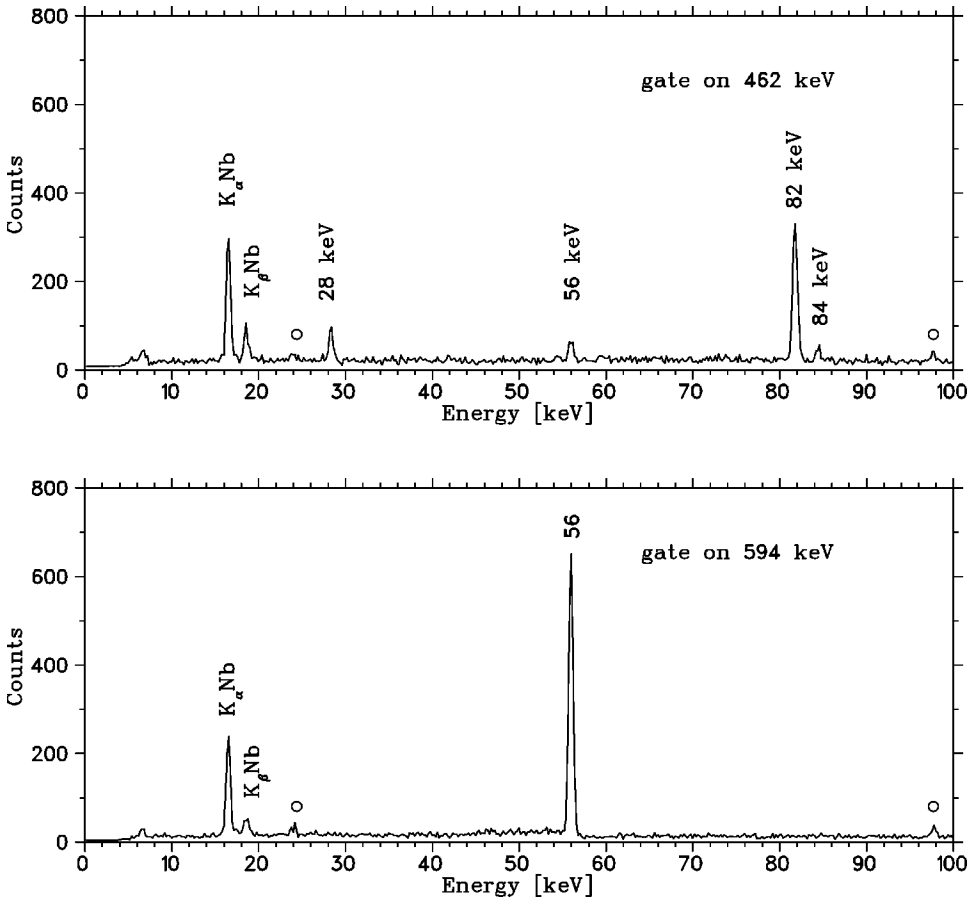

FIG. 1. Low-energy part of projected spectra of the x-ray detector gated by the 462 and 594 keV γ rays. The weak peak at 24 keV (open circle) could be due to a transition in the level scheme of ^{99}Nb (see text). The other open circle marks the 98 keV transition (^{99}Mo) due to random coincidences. The area of the 56 keV peak in the 462 keV gate is proportional to the $\gamma + e^-$ intensity of the 28 keV transition. The 594 keV gate is used for normalization of the 56 keV peak area.

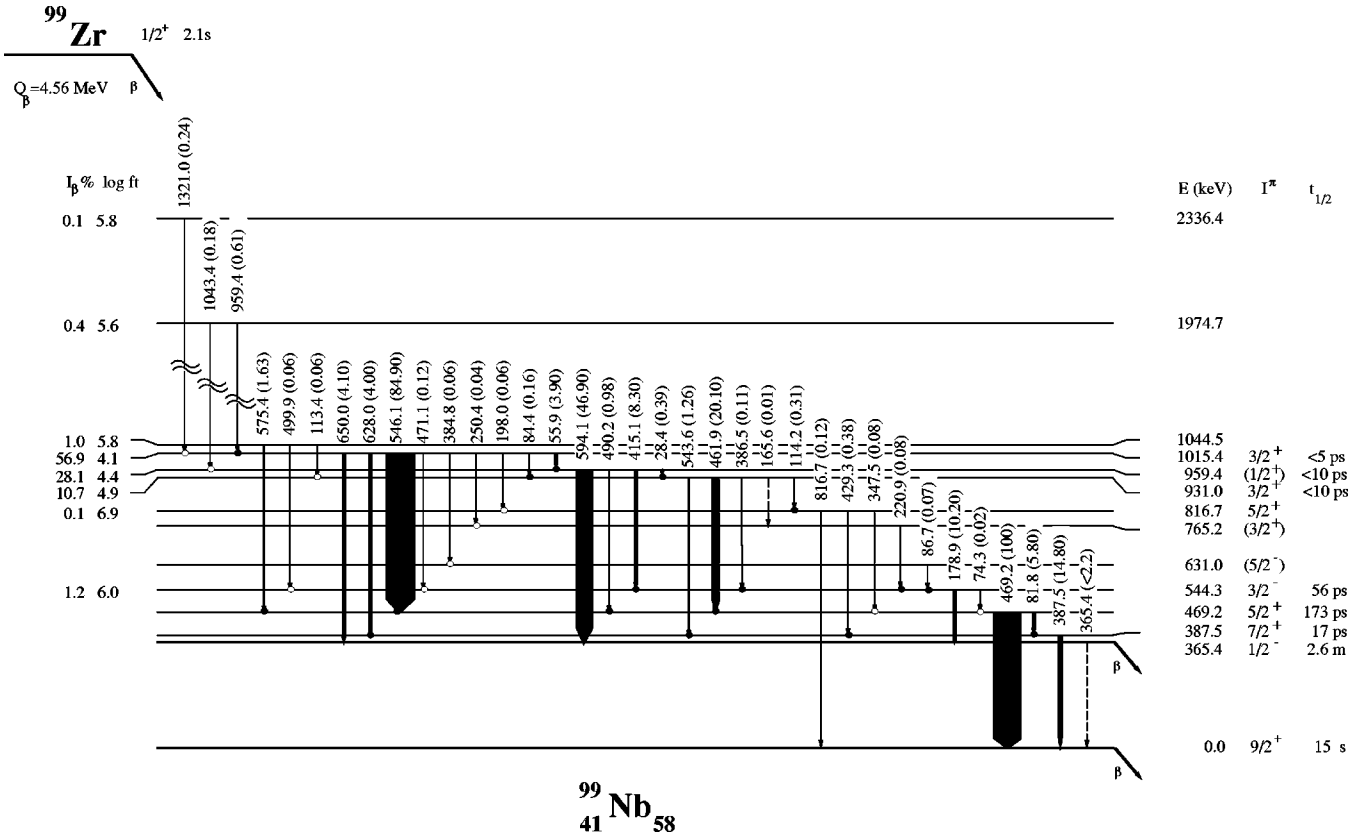

FIG. 2. Decay scheme of ^{99}Zr to ^{99}Nb from this work and data compiled in Ref. [29].

suggests $I^{\pi}(959)=1/2^{+}$. This new assignment implies $E2$ character for the weak 490 keV transition to the 469 keV level, for which the deduced enhancement of >1.2 still can be low enough. Thus, although not unique, this assignment is the most logical one and we will adopt it through the subsequent discussion.

TABLE III. Levels populated in ^{99}Nb by β decay of ^{99}Zr. The branching of the first-forbidden β feeding to the $1/2^{-}$ was assumed to be less than 1.0% ($\log ft=5.9$). $\log ft$ values are calculated using $T_{1/2}(^{99}\mathrm{Zr})=2.1$ s and $Q_{\beta}=4.54$ MeV [29]. Level lifetimes are from [28,29].

Energy (keV)	β feeding %	$\log ft$	$t_{1/2}$ [ps]	I^{π}
0.0	0			$9/2^{+}$ [29]
365.4 (2)	0.6 (32)	5.9		$1/2^{-}$ [29]
387.5 (2)	0.4 (15)	6.6	17 (4)	$7/2^{+}$ [29]
469.2 (2)	0.4 (39)	6.5	173 (4)	$5/2^{+}$ [29]
544.3 (3)	1.2 (10)	6.0	56 (10)	$3/2^{-}$ [29]
631.0 (4)	0.01 (2)			$5/2^{-}$ [29]
765.2 (4)	0.02 (1)	7.8		$3/2^{+}$ [29]
816.7 (2)	0.12 (7)	6.9		$5/2^{+}$ [29]
931.0 (2)	10.7 (14)	4.9	<10	$3/2^{+}$
959.4 (2)	28.1 (30)	4.4	<10	$(1/2^{+})$
1015.4 (1)	56.9 (40)	4.1	<5	$3/2^{+}$ [29]
1044.5 (2)	0.98 (25)	5.8		(1/2,3/2)
1974.7 (3)	0.44 (8)	5.6		$(1/2,3/2)^{+}$ [29]
2336.4 (3)	0.13 (4)	5.8		(1/2,3/2)

The 544.3 keV level has been assigned $I^{\pi}=3/2^{-}$ by various authors [29]. This is consistent with the $M1$ multipolarity obtained from the conversion coefficient of the 179 keV transition to the $1/2^{-}$ isomer (see Table II). The new 74.3 keV transition, represents an alternative $E1$ decay to the 469 keV $5/2^{+}$ level.

Other levels are only very weakly fed and no lifetime measurements are available. The 631.0 keV level is fed via the γ ray of 384.8 keV from the $3/2^{+}$ level at 1015 keV and it decays by the 86.7 keV transition to the $3/2^{-}$ level at 544 keV. These transitions and the weakness of direct β feeding leave several assignments open, but consistent with $I^{\pi}(631)=5/2^{-}$ reported in the (t,α) study of Flynn *et al.* [37]. An $E2$ decay to the $1/2^{-}$ isomer cannot be observed, possibly due to the poorer detection limit in the singles spectra.

The 765.2 keV level is placed by the clear cascade of the 250.4 and 220.9 keV transitions, the latter being slightly more intense. This level was also reported in [37] and assigned $I^{\pi}=3/2^{+}$, which indeed is possible from the transitions. The β feeding is very weak compared to those of the above discussed $3/2^{+}$ states.

The 816.7 keV level was reported in β decay by Pfeiffer *et al.* [30], but not included in the Nuclear Data Sheets evaluation, and in two reaction studies [37,41] which proposed $I^{\pi}=5/2^{+}$. There is a 114 keV transition from the $3/2^{+}$ state at 931 keV, the lifetime limit [28] and conversion coefficient (see Table II) of which, favor M1 character. Thus, the decay data are consistent with the above stated $I^{\pi}(817)=5/2^{+}$ assignment.

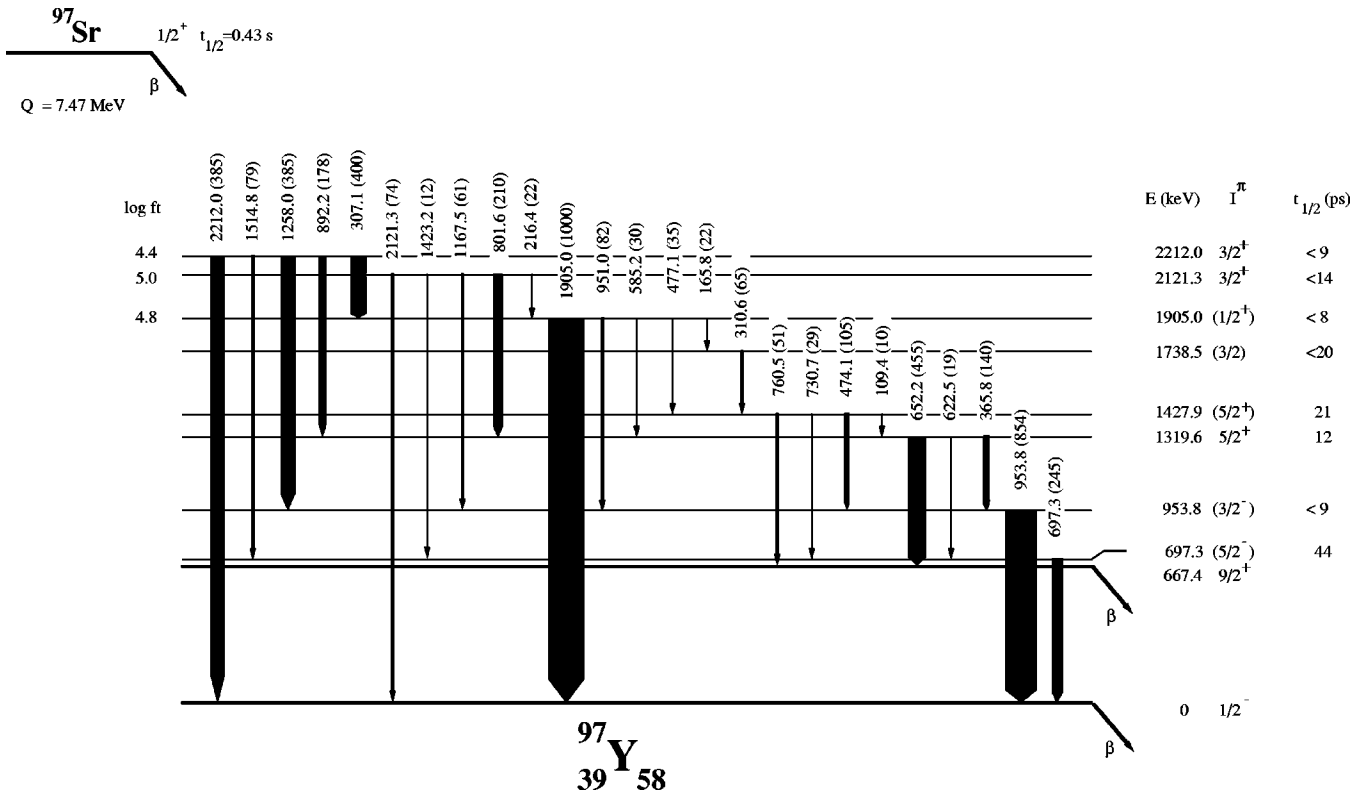

FIG. 3. Partial decay scheme of ^{97}Sr based on Refs. [10,27]. Only the levels discussed in the text are shown. The new transitions of 165.8 and 730.7 keV are included and some spin assignments, as discussed in the text, have been modified.

The 1044.5 keV level is a new level. The 575–469 keV cascade occurs, but in reverse order, in the level scheme of ^{99}Zr [15]. Nevertheless, there is no doubt for the placement of a level in ^{99}Nb since the 575 keV line is seen also in the 82 and 387 keV gates. The logft value is 5.8. Thus, $I^{\pi}=1/2^{+}$ and $3/2^{\pm}$ are possible, with even parity being more probable.

The two high-lying levels at 1974.6 and 2336.3 keV are rather weakly fed in β decay. It was mentioned that the present experiments cannot rule out the existence of high-energy transitions with intensities of the order of up to 1 relative intensity unit that would depopulate levels directly to the $1/2^{-}$ isomer. This means that the β feedings to the 1975 and 2336 keV levels shown in Table III are lower limits and some $1/2^{+}$, $3/2^{+}$ levels may have remained unobserved. Nevertheless, in spite of a possible shift of the distribution of β strength to higher excitation energies, it remains that the levels at 931, 959, and 1015 keV are very strongly fed directly in β decay.

C. New transitions and revised spin assignments in ^{97}Y

The γ-γ data from our previous experiments [20,24] reveal the existence of two new transitions in the level scheme of ^{97}Y. A partial level scheme, relevant for the present discussion, is shown in Fig. 3. It is basically the one established by Pfeiffer *et al.* [27]. The level lifetimes later measured by Büscher *et al.* [10] provide a limit to the multipolarities of most of the transitions.

A new transition of 730.7(5) keV and $I_{\gamma}=29(6)$, using the normalization $I_{\gamma}(1905)=1000$ from Ref. [27], is placed between the 1428 and 697 keV levels, owing to a coincidence with the 697.3 keV γ ray and coincidences between the 310.6 keV (1739→1428) and 697.3 keV (697→g.s.) lines. According to previously available information the 1428 keV level could be a $5/2^{+}$ or a $7/2^{+}$ state and it was discussed as a $7/2^{+}$ state by Büscher *et al.* [10]. The new decay branch to the 697 keV $3/2^{-}$ state, however, results in the unique $I^{\pi}(1428)=5/2^{+}$ assignment. We subsequently present arguments supporting the exchange of the low-lying $3/2^{-}$ and $5/2^{-}$ levels, but this does not modify this conclusion.

The other new 165.8(6) keV transition, with $I_{\gamma}=22(8)$, has coincidences with the γ rays of 307.1 keV (2012 →1905) and 310.6 keV (1739→1428). Hence, it fits between the 1905 and 1739 keV levels. With the new assignments $I^{\pi}(1905)=1/2^{+}$ (discussed in the following) and $I^{\pi}(1428)=5/2^{+}$, and the dipole character of the connecting transitions, the 1739 keV level has $I=3/2$. Unfortunately, the revised logft value of 6.1 does not indicate the parity.

The β decay of $I^{\pi}=1/2^{+}$ ^{97}Sr to ^{97}Y has three strong branches, of clearly allowed character, to the levels at 1905, 2121, and 2212 keV. Pfeiffer *et al.* did not report a value for the first-forbidden β branch to the $1/2^{-}$ ground state [27]. Nevertheless, only a 5% branching is obtained assuming the logft value of 5.9, so that this is of little consequence on the strong branchings. The 2121 and 2212 keV levels, which decay to both $3/2^{-}$ and $5/2^{-}$ states are thus $3/2^{+}$ states. By analogy with the decay of ^{99}Zr to ^{99}Nb, it is tempting to assign $I^{\pi}=1/2^{+}$ to the other strongly β-fed level at 1905 keV. We note that $I^{\pi}=1/2^{+}$ was excluded by the transition of 477.1 keV to the 1428 keV level, as long as this latter was assigned $I^{\pi}=7/2^{+}$. The favored decay mode of the 1905 keV

level is to the $1/2^-$ ground state while the transition to the 1320 keV ($I^\pi=5/2^+$) level is rather weak. This looks very similar to the decay of the $1/2^+$ state at 959 keV in ^{99}Nb. An inconsistency is, however, the presence of a decay to the 954 keV level ($I_\gamma=82$) discussed as a $5/2^-$ state by Büscher *et al.* [10] but not to the 697 keV (presumably $3/2^-$) level. In our analysis the latter decay branch could not be found, the intensity being estimated to $I_\gamma<30$. The inconsistency can be removed by exchanging the positions of the $3/2^-$ and $5/2^-$ states, with respect to Ref. [10]. Then, the transition to the 954 keV level becomes an $E1$, whereas the nonobserved one to the 697 keV level would have to be a $M2$ (the single-particle estimate corresponds to five units, which is still below the detection limit of the experiments). As a matter of fact, there is no strong experimental evidence for favoring one or the other assignment for the 697 and 954 keV levels. Pfeiffer *et al.* [27] favored the placement of the $5/2^-$ level as the highest one and this also yields a reasonable $E2$ enhancement for the 954 keV $5/2^-$ to $1/2^-$ transition [10]. Nevertheless, a mere quadratic extrapolation of the excitation energies in the isotopes ^{91}Y, ^{93}Y, and ^{95}Y [34] leads to values of 941 keV ($3/2^-$) and 777 keV ($5/2^-$), placing $5/2^-$ indeed below the $3/2^-$ level in ^{97}Y. A more meaningful argument is that the 954 keV level is more strongly populated by γ-ray cascades (854 intensity units) than the 697 keV level (245 units) [27]. It seems logical that, in the decay of the $I^\pi=1/2^+$ level, a $3/2^-$ level receives more feeding than a $5/2^-$ level. To summarize, $I^\pi(1905)=1/2^+$ is the most natural assignment for this level and the required exchange of the the $3/2^-$ and $5/2^-$ levels is not in conflict with the experimental data. This opens the possibility of finding even more analogies between the decays of ^{97}Sr and ^{99}Zr, which will be dicussed in the next section.

IV. CALCULATIONS OF LEVEL STRUCTURE OF ^{99}Nb

A. Interacting boson-fermion plus broken-pair model calculation

In the systematic investigations of nuclei near the $Z=40$, $N=56$ subshell closures the nucleus ^{97}Y has been recently investigated experimentally and described theoretically in the interacting boson-fermion plus broken-pair model (IBFBPM) [26]. Details about the interacting boson model and its successive extensions up to the inclusion of broken pairs can be found in Refs. [42–55]. In this paper we extend the IBFBPM treatment to the ^{99}Nb nucleus, with two additional protons in comparison to ^{97}Y. The IBFBPM configuration space of an odd-even nucleus with $2N+1$ valence nucleons comprises components of the type [26,55]

$$|N\ \ bosons\otimes 1\ \ fermion\rangle + |(N-1)\ \ bosons\otimes 1\ \ broken\ pair\otimes 1\ \ fermion\rangle. \tag{4.1}$$

As in the calculation for ^{97}Y, we include broken neutron pairs. The boson-fermion basis states thus contain one-quasiproton-two-quasineutron states in addition to one-quasiproton states. The main difference in the IBFBPM parametrization for ^{99}Nb with respect to ^{97}Y is given by energies and occupation probabilities of quasiprotons, due to the two additional protons in the valence shell. For ^{99}Nb the BCS occupation probabilities and quasiparticle energies for the $\pi\tilde{g}_{9/2}$, $\pi\tilde{p}_{1/2}$, $\pi\tilde{p}_{3/2}$, $\pi\tilde{f}_{5/2}$, $\pi\tilde{d}_{5/2}$ quasiparticles are $v^2=$ 0.13, 0.92, 0.97, 0.98, 0.01 and $E=1.04$, 1.37, 1.54, 1.85, 7.04 MeV, respectively. The main difference between quasiparticle states in ^{99}Nb and ^{97}Y is in the relative positions of the $\pi\tilde{g}_{9/2}$ and $\pi\tilde{p}_{1/2}$ quasiparticles: in ^{97}Y the $\pi\tilde{p}_{1/2}$ quasiparticle lies below $\pi\tilde{g}_{9/2}$, and in ^{99}Nb $\pi\tilde{p}_{1/2}$ lies above $\pi\tilde{g}_{9/2}$. In analogy to the previous IBFBPM calculation for ^{97}Y [26], the $\pi\tilde{d}_{5/2}$ configuration from the shell above the valence shell is added because of the large non-spin-flip matrix element $\langle \pi d_{5/2}\|Y_2\|\pi g_{9/2}\rangle$. All the other IBFBPM parameters are taken to be the same as in the previous calculation for ^{97}Y, except for small modifications of the boson parameter h_1 to 0.715 MeV and of the boson-fermion monopole interaction strength A_0^π for negative parity states to 0.06 MeV.

The IBFBPM Hamiltonian is diagonalized in the boson-fermion basis (4.1) and we obtain the energy spectra and the wave functions:

$$|J_k^\pi\rangle=\sum_{j n_d v R;J}\xi_{j,n_d v R;J}|\pi\tilde{j},n_d v R;J\rangle + \sum_{jj'j''I_{\nu\nu}I_{\pi\nu\nu},n_d v R;J}\eta_{jj'j''I_{\nu\nu}I_{\pi\nu\nu},n_d v R;J} \times|[\pi\tilde{j},(\nu\tilde{j}',\nu\tilde{j}'')I_{\nu\nu}]I_{\pi\nu\nu},n_d v R;J\rangle. \tag{4.2}$$

Here $\pi\tilde{j}$ stands for proton quasiparticle, $\nu\tilde{j}'$ and $\nu\tilde{j}''$ for neutron quasiparticles. In the boson part of the basis states, the n_d d bosons are coupled to the total boson angular momentum R. The number of s bosons associated with the boson state $|n_d v R\rangle$ is $n_s=N-n_d$ where N is the total number of s and d bosons. In Fig. 4 we present the calculated energy spectrum of ^{99}Nb in comparison to the available data and Table IV displays the sizeable components in the wave functions of some states.

Using the IBFBPM wave functions we calculate the $E2$ and $M1$ electromagnetic properties of ^{99}Nb, taking the effective boson charge $e^{\rm vib}=1$, proton gyromagnetic ratio $g_s^\pi=0.4\ g_s^{\pi,\rm free}$ and the other values of effective charges and gyromagnetic ratios as used in the previous IBFBPM calculation for ^{97}Y. The calculated $E2$ and $M1$ transitions for low-lying states are given in Table V and the half-lives in Table VI.

B. Microscopic quasiparticle phonon model calculation

The microscopic quasiparticle phonon model (MQPM) was introduced in Refs. [56,57]. The present calculation follows the procedure used for calculation of decay properties of ^{99}Nb and level structure of ^{99}Mo [21]. In our MQPM calculation we use essentially the Coulomb-corrected Woods-Saxon single-particle energies with the parametrization of Ref. [58]. The neutron and proton single-particle basis consist of the p-f and s-d-g oscillator major shells complemented by the intruder orbital $0h_{11/2}$ from the next oscillator major shell. The monopole matrix elements of the two-body interaction are scaled by pairing-strength param-

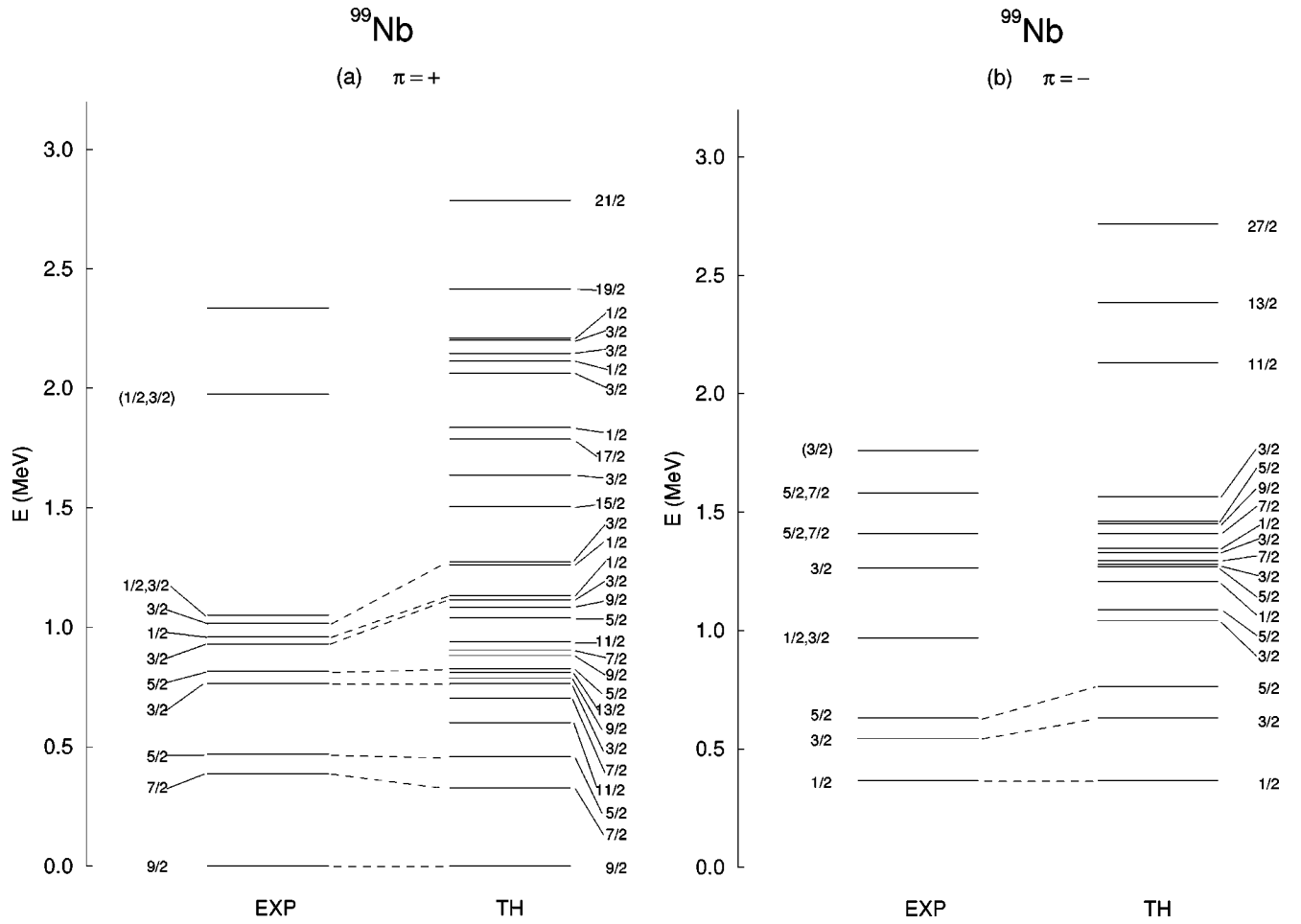

FIG. 4. Calculated IBFBPM states in ^{99}Nb of (a) positive parity, and (b) negative parity in comparison to the available data. For positive parity the states presented are: all states up to 1.1 MeV; all $1/2^+$, $3/2^+$ states and yrast states for $I^\pi \geq 15/2^+$ in the energy interval 1.1 − 2.2 MeV; and yrast states in the energy interval 2.2 − 2.8 MeV. For negative-parity the states presented are all states up to 1.6 MeV; and only yrast states in the energy interval 2.2 − 2.8 MeV.

eters [59], by comparison with semiempirical pairing gaps obtained from proton and neutron separation energies. The low-lying states of odd-A nuclei are composed of various quasiparticles coupled to the few lowest and most important excitations of an even-even core reference nucleus of mass $A-1$ constructed using the QRPA method of Ref. [60]. The truncation of three-quasiparticle model space is controlled by looking at the convergence of the odd-A spectrum versus the number of included RPA excitations. The odd nuclei ^{99}Zr and ^{99}Nb were constructed by, respectively, adding a neutron and a proton quasiparticle to the reference nucleus ^{98}Zr. This makes it possible to describe the β decay of ^{99}Zr to levels in ^{99}Nb. However, as in the case of the IBFBPM, the experimental excitation spectrum of ^{100}Mo was used as the guide line when determining the phonon energies in the QRPA calculation. The results obtained for the $1/2^+$ and $3/2^+$ states in ^{99}Nb and the corresponding calculated logft values for the decay of the $1/2^+$ ground state of ^{99}Zr into these states are shown in Table VII.

V. DISCUSSION

A. Nuclear structure of ^{99}Nb in IBFBPM

The region of $A \approx 100$ nuclei has been discussed in the framework of the interacting boson model in Refs. [9,13,17,22,25,26].

As already pointed out, the $\pi\tilde{g}_{9/2}$ and $\pi\tilde{p}_{1/2}$ quasiproton states exchange their positions between ^{97}Y and ^{99}Nb. Thus, in ^{97}Y the $1/2^-$ level is the ground state whereas the $9/2^+$ level is the isomeric state, while in ^{99}Nb the situation is the opposite. The nature of these states is the same as in the previous calculation for ^{97}Y [26], i.e., the largest components in the wave functions of the $9/2^+_1$ and $1/2^-_1$ states are the $\pi\tilde{g}_{9/2}$ and $\pi\tilde{p}_{1/2}$ quasiparticle components, respectively.

The next lowest-lying even parity states in ^{99}Nb are built on the $\pi\tilde{g}_{9/2} \otimes 2^+_1$ configuration, producing a multiplet with $I = 5/2^+, \ldots, 13/2^+$. In the IBFBPM calculation an effective core is used, lying between ^{100}Mo with $E(2^+_1) = 535$ keV and ^{98}Zr with $E(2^+_1) = 1223$ keV, but much closer to ^{100}Mo. Thus, the $7/2^+_1$ (387 keV) and the $5/2^+_1$ (469 keV) levels are the members of this multiplet with the lowest spins, in accordance with their strong population by γ-ray cascades after β-decay of the ^{99}Zr $1/2^+$ ground state. These states are based on the $\pi\tilde{g}_{9/2}$-one-d-boson multiplets. From the present coincidence data, the existence of two additional levels at 363 and 379 keV has been speculated, having a link to the $7/2^+$ 387 keV level, which could have the $I = 9/2$ and 11/2 assignments and therefore be associated with other members of the $\pi\tilde{g}_{9/2} \otimes 2^+_1$ multiplet. However, the remaining three

TABLE IV. Components in the IBFBPM wave functions of some low-lying states in ^{99}Nb. Only the components with amplitudes larger than 1% are shown. Boson states with seniority $v > v_{\text{lowest}}$ are denoted by n_d R'.

I_k^π	$\pi\tilde{j}$ or $[\pi\tilde{j},(\nu\tilde{j}',\nu\tilde{j}'')I_{\nu\nu}]I_{\pi\nu\nu}$	n_d	R	ξ
$9/2_1^+$	$\pi g_{9/2}$	0	0	0.90
	$\pi g_{9/2}$	1	2	−0.39
$7/2_1^+$	$\pi g_{9/2}$	1	2	−0.91
	$\pi g_{9/2}$	2	2	−0.14
	$\pi g_{9/2}$	2	4	0.27
	$[\pi g_{9/2},(\nu s_{1/2},\nu d_{5/2})2]7/2$	0	0	−0.15
$1/2_1^-$	$\pi p_{1/2}$	0	0	0.77
	$\pi p_{1/2}$	2	0	0.15
	$\pi p_{3/2}$	1	2	−0.40
	$\pi p_{3/2}$	2	2	−0.16
	$\pi f_{5/2}$	1	2	−0.39
	$\pi f_{5/2}$	2	2	−0.15
$5/2_1^+$	$\pi g_{9/2}$	1	2	0.77
	$\pi g_{9/2}$	2	2	−0.56
	$\pi g_{9/2}$	2	4	0.16
	$\pi g_{9/2}$	3	3	−0.11
$3/2_1^-$	$\pi p_{1/2}$	1	2	0.49
	$\pi p_{1/2}$	2	2	0.19
	$\pi p_{3/2}$	0	0	0.67
	$\pi p_{3/2}$	1	2	0.34
	$\pi p_{3/2}$	2	0	0.10
	$\pi p_{3/2}$	2	2	0.16
	$\pi f_{5/2}$	1	2	−0.16
	$\pi f_{5/2}$	2	4	−0.22
$11/2_1^+$	$\pi g_{9/2}$	1	2	0.85
	$\pi g_{9/2}$	2	2	0.38
	$\pi g_{9/2}$	2	4	−0.20
	$[\pi g_{9/2},(\nu s_{1/2},\nu d_{5/2})2]11/2$	0	0	0.18
$5/2_1^-$	$\pi p_{1/2}$	1	2	0.58
	$\pi p_{1/2}$	2	2	0.18
	$\pi p_{3/2}$	1	2	−0.18
	$\pi p_{3/2}$	2	4	−0.26
	$\pi p_{3/2}$	3	4	−0.12
	$\pi f_{5/2}$	0	0	−0.55
	$\pi f_{5/2}$	1	2	−0.27
	$\pi f_{5/2}$	2	0	−0.10
	$\pi f_{5/2}$	2	2	−0.19
	$\pi f_{5/2}$	2	4	−0.15
	$[\pi p_{1/2},(\nu s_{1/2},\nu d_{5/2})2]5/2$	0	0	0.10
$3/2_1^+$	$\pi g_{9/2}$	2	4	0.31
	$\pi g_{9/2}$	3	3	0.84
	$\pi g_{9/2}$	3	4	−0.24
	$\pi g_{9/2}$	4	4	0.15
	$\pi g_{9/2}$	4	5	−0.13
	$[\pi g_{9/2},(\nu s_{1/2},\nu d_{5/2})2]7/2$	2	2	−0.16
$9/2_2^+$	$\pi g_{9/2}$	0	0	0.26
	$\pi g_{9/2}$	1	2	0.45
	$\pi g_{9/2}$	2	0	−0.13
	$\pi g_{9/2}$	2	2	0.59
	$\pi g_{9/2}$	3	0	−0.42
	$\pi g_{9/2}$	3	3	0.21
	$[\pi g_{9/2},(\nu s_{1/2},\nu d_{5/2})2]9/2$	0	0	0.14
	$[\pi g_{9/2},(\nu s_{1/2},\nu d_{5/2})2]11/2$	1	2	0.13
$13/2_1^+$	$\pi g_{9/2}$	1	2	−0.91
	$\pi g_{9/2}$	2	2	0.21
	$\pi g_{9/2}$	2	4	0.26
	$[\pi g_{9/2},(\nu s_{1/2},\nu d_{5/2})2]13/2$	0	0	−0.16
$5/2_2^+$	$\pi g_{9/2}$	1	2	0.48
	$\pi g_{9/2}$	2	2	0.47
	$\pi g_{9/2}$	2	4	−0.66
	$[\pi g_{9/2},(\nu s_{1/2},\nu d_{5/2})2]5/2$	0	0	0.11
	$[\pi g_{9/2},(\nu s_{1/2},\nu d_{5/2})2]7/2$	1	2	−0.15
$3/2_2^+$	$\pi g_{9/2}$	2	4	−0.49
	$\pi g_{9/2}$	3	3	0.11
	$\pi g_{9/2}$	3	4	0.33
	$\pi g_{9/2}$	4	4	0.59
	$\pi g_{9/2}$	4	5	−0.42
	$[\pi g_{9/2},(\nu s_{1/2},\nu d_{5/2})2]7/2$	3	3	−0.11
$1/2_1^+$	$\pi g_{9/2}$	2	4	0.32
	$\pi g_{9/2}$	3	4	−0.29
	$\pi g_{9/2}$	4	4	−0.11
	$\pi g_{9/2}$	4	4′	−0.73
	$\pi g_{9/2}$	4	5	0.41
	$[\pi g_{9/2},(\nu s_{1/2},\nu d_{5/2})2]7/2$	3	3	0.14
$3/2_3^+$	$\pi g_{9/2}$	2	4	0.67
	$\pi g_{9/2}$	3	3	−0.39
	$\pi g_{9/2}$	4	4	0.40
	$\pi g_{9/2}$	4	5	−0.34
	$[\pi g_{9/2},(\nu s_{1/2},\nu d_{5/2})2]5/2$	1	2	0.15

calculated members of this multiplet, $11/2_1^+$, $9/2_2^+$, and $13/2_1^+$ lie at a few hundred keV higher in energy. Therefore, it seems more probable to assume that these two states, if they actually exist, are associated with intruder states. A $9/2^+$ level, although probably at a somewhat higher energy, could be produced by coupling the low-lying intruder 0^+ core state, at 854 keV in ^{98}Zr and and 695 keV in ^{100}Mo [34], to the $\tilde{g}_{9/2}$ proton. Therefore, other even-parity levels may exist in this energy range, but β decay from a $1/2^+$ state is not appropriate for their observation.

The weakly populated $3/2^+$ and $5/2^+$ levels at 765 and 817 keV are quite lower than the 2_2^+ and 4_1^+ levels in the core, but they are very close to the calculated $3/2_1^+$ and $5/2_2^+$ states, which are based on the $|\pi\tilde{g}_{9/2},33;3/2\rangle$ and

TABLE V. Calculated $E2$ and $M1$ transitions between some low-lying states in comparison to data for ^{99}Nb.

$I_i \to I_f$ $(\hbar)(\hbar)$	$B(E2)$ (e^2b^2) IBFBPM	$B(M1)$ (μ_N^2) IBFBPM	I_γ Expt.	I_γ IBFBPM
$7/2_1^+ \to 9/2_1^+$	0.0135	0.0842 [a]	100	100
$5/2_1^+ \to 7/2_1^+$	0.0131	0.1308	6	20
$\to 9/2_1^+$	0.0224		100	100
$3/2_1^- \to 1/2_1^-$	0.0364	0.1036	100	100
$5/2_1^- \to 3/2_1^-$	0.0087	0.0046	100	100
$\to 1/2_1^-$	0.0402		[b]	1216
$3/2_1^+ \to 5/2_1^+$	0.0107	0.0022		100
$\to 7/2_1^+$	0.0051			37
$5/2_2^+ \to 3/2_1^+$	0.0025	0.0451		0.02
$\to 5/2_1^+$	0.0028	0.0103	21	2
$\to 7/2_1^+$	0.0100	0.3585	100	100
$\to 9/2_1^+$	0.0049		32	4
$3/2_2^+ \to 5/2_2^+$	0.0003	0.2802	2	29
$\to 3/2_1^+$	0.0071	0.0006	0.05	0.2
$\to 5/2_1^+$	0.0092	0.0135	100	100
$\to 7/2_1^+$	0.0030		6	7
$1/2_1^+ \to 3/2_2^+$	0.0015	1.789 [c]	40	34
$\to 5/2_2^+$	0.0034			0.1
$\to 3/2_1^+$	0.0062	0.00004		1.2
$\to 5/2_1^+$	0.0062		100 [d]	100
$3/2_3^+ \to 1/2_1^+$	0.000005	0.0574	5	0.2
$\to 3/2_2^+$	0.00002	0.0425	0.2	0.4
$\to 5/2_2^+$	0.0057	0.4363	0.07	58
$\to 3/2_1^+$	0.0013	0.0971	0.05	26
$\to 5/2_1^+$	0.0073	0.0348	100	100
$\to 7/2_1^+$	0.0043		5	5

[a]The measured value for the 387 keV transition is 0.039(11) from Ref. [28].

[b]It is possible that the transition even with such a large branch is not seen experimentally (see text).

[c]The measured value for the 28 keV transition is $> 0.7\ \mu_N^2$ from Ref. [28].

[d]It should be noted that the transition of 490 keV represents only 2 and 12 % of the strengths of the $E1$ transitions to the $1/2_1^-$ and $3/2_1^-$ states, respectively.

TABLE VI. Calculated lifetimes of some states in comparison to data [28] for ^{99}Nb.

I_k^π $(\hbar)$	$T_{1/2}$ (ns) Expt.	$T_{1/2}$ (ns) IBFBPM
$7/2_1^+$	0.017 (4)	0.008
$5/2_1^+$	0.173 (4)	0.088
$3/2_1^-$	0.56 (10)	0.063
$5/2_1^-$		0.966 [a]
$3/2_1^+$		$\ll 0.39$ [b]
$5/2_2^+$		0.001
$3/2_2^+$	< 0.010	0.019
$1/2_1^+$	< 0.010	0.005 [c]
$3/2_3^+$	< 0.005	0.004

[a]The half-life is reduced to 0.22 ns by including a tensor term in the $M1$ operator (see text).

[b]This is an estimate for the upper limit, because only the $E1$ transition to the $3/2_1^-$ state was observed, although a strong branch to the $1/2_1^-$ level is predicted.

[c]Obtained by assuming that 94% of the decay intensity goes to odd-parity states.

$|\pi\tilde{g}_{9/2}, 24; 5/2\rangle$ components, respectively, as the largest components in the corresponding wave functions. The decay of the 765 keV level by a single transition to the $3/2^-$ level at 544 keV is difficult to be interpreted and this could mean that, e.g., the transition to the $1/2^-$ isomer was overlooked. We note that the decay pattern of the $5/2_2^+$ state, associated with the 817 keV level, to the $5/2_1^+$ and $7/2_1^+$ states, resembles the $\Delta n_d = 1$ pattern. The main components in the wave functions of the $5/2_2^+$, $5/2_1^+$, and $7/2_1^+$ states are in accordance with this expectation.

The odd-parity $3/2^-$ (544 keV) and $5/2^-$ (631 keV) levels are seen in proton pickup reactions [37], which indicates important amplitudes of the $p_{3/2}$ and $f_{5/2}$ proton holes instead of the $p_{1/2} \otimes 2^+$ couplings. The calculated low-lying negative-parity triplet states $1/2^-$, $3/2^-$, and $5/2^-$ are based on the $\pi\tilde{p}_{1/2}$, $\pi\tilde{p}_{3/2}$, and $\pi\tilde{f}_{5/2}$ quasiparticles, respectively. The hole-type character of the $3/2_1^-$ and $5/2_1^-$ states is in accordance with the proton pickup data. The same interpretation is made for the $3/2^-$ and $5/2^-$ levels in ^{97}Y after exchanging their positions (see Sec. V C). In the IBFBPM calculation, for realistic parametrizations, we cannot obtain the lowest $3/2^-$ and $5/2^-$ states being dominated by $p_{1/2} \otimes 2^+$ core+particle coupling that was proposed in Ref. [10].

The agreement between the calculated and experimental electromagnetic transitions presented in Table V is reasonable. We note that the decay of the $5/2_1^-$ state requires additional clarification regarding the strongest calculated branch in comparison to experiment. Namely, the calculated $5/2_1^- \to 1/2_1^-$ transition is an order of magnitude stronger than the calculated $5/2_1^- \to 3/2_1^-$ transition, while experimentally there is no information available on the $5/2_1^- \to 1/2_1^-$ transition. However, it was mentioned previously that the limit of detection for this kind of transition, as a result of the isomeric character of the $1/2^-$ level, is rather high. Thus, we cannot exclude the possibility that the experimental $5/2_1^- \to 1/2_1^-$ transition is present and even stronger than the $5/2_1^- \to 3/2_1^-$ transition. Furthermore, we note that the $5/2_1^- \to 3/2_1^-$ transition is l forbidden in the leading order, leading to a small $B(M1)$ value. Therefore, a sizable contribution may be due to the tensor term in the $M1$ operator, which was previously included in some IBFM calculations [61,62]. Since the contribution of broken pairs to these two transitions is small, we can estimate a possible influence of the tensor term by performing the standard IBFM calculation with the gyromagnetic ratio $g_T^\pi = \frac{1}{20}\, g_s^{\pi,\text{free}} \langle r^2 \rangle = 5.164$, which gives $B(M1)$ $(5/2_1^- \to 3/2_1^-) = 0.17 \mu_N^2$. In this case the intensity ratio of the $5/2_1^- \to 3/2_1^-$ and $5/2_1^- \to 1/2_1^-$ transitions is 100/33. Thus, by including the tensor term in the $M1$ operator the two branches depopulating the $5/2_1^-$ state become comparable, which comes closer to the experimental branchings.

We note that the largest calculated $B(M1)$ value is obtained for the $1/2_1^+ \to 3/2_2^+$ transition. This is in accordance with the strong branch observed for the 28 keV transition in

TABLE VII. Structure of the $1/2^+$ and $3/2^+$ states of ^{99}Nb and logft values for population in decay of the $1/2^+$ ground state of ^{99}Zr calculated in the MQPM. For comparison with the IBFBPM the $\tilde{g}_{9/2}\otimes 2_1^+$ multiplet is also shown. The first four largest components are listed unless smaller than 1%.

I_k^π	E(MeV)	logft	Structure			
$9/2_1^+$	0.00		$0.93\ \tilde{g}_{9/2}$	$-0.31\ \tilde{g}_{9/2}\otimes 2_1^+$	$-0.13\ \tilde{g}_{9/2}\otimes 4_1^+$	$+0.03\ \tilde{d}_{5/2}\otimes 2_1^+$
$7/2_1^+$	0.38		$0.98\ \tilde{g}_{9/2}\otimes 2_1^+$	$+0.10\ \tilde{g}_{9/2}\otimes 4_1^+$	$+0.02\ \tilde{g}_{9/2}\otimes 4_2^+$	$-0.02\ \tilde{p}_{1/2}\otimes 3_1^-$
$5/2_1^+$	0.46		$0.99\ \tilde{g}_{9/2}\otimes 2_1^+$	$+0.07\ \tilde{p}_{1/2}\otimes 3_1^-$	$-0.06\ \tilde{g}_{9/2}\otimes 4_1^+$	$+0.04\ \tilde{d}_{5/2}$
$13/2_1^+$	0.49		$1.00\ \tilde{g}_{9/2}\otimes 2_1^+$	$-0.07\ \tilde{g}_{9/2}\otimes 4_1^+$	$-0.02\ \tilde{g}_{9/2}\otimes 6_1^+$	$-0.02\ \tilde{g}_{9/2}\otimes 6_2^+$
$9/2_2^+$	0.52		$0.95\ \tilde{g}_{9/2}\otimes 2_1^+$	$+0.32\ \tilde{g}_{9/2}$	$+0.03\ \tilde{g}_{9/2}\otimes 4_1^+$	$+0.02\ \tilde{g}_{9/2}\otimes 6_1^+$
$11/2_1^+$	0.53		$1.00\ \tilde{g}_{9/2}\otimes 2_1^+$	$-0.11\ \tilde{g}_{9/2}\otimes 4_1^+$	$-0.03\ \tilde{g}_{9/2}\otimes 4_2^+$	$+0.01\ \tilde{g}_{9/2}\otimes 4_3^+$
$3/2_1^+$	0.95	5.0	$0.98\ \tilde{g}_{9/2}\otimes 4_1^+$	$+0.06\ \tilde{g}_{9/2}\otimes 4_2^+$	$+0.03\ \tilde{f}_{5/2}\otimes 3_1^-$	$-0.03\ \tilde{g}_{9/2}\otimes 4_3^+$
$1/2_1^+$	1.04	4.1	$1.00\ \tilde{g}_{9/2}\otimes 4_1^+$	$-0.10\ \tilde{g}_{9/2}\otimes 4_2^+$	$-0.05\ \tilde{s}_{1/2}$	$-0.04\ \tilde{f}_{5/2}\otimes 3_1^-$
$3/2_2^+$	1.35	4.5	$0.99\ \tilde{g}_{9/2}\otimes 4_2^+$	$-0.07\ \tilde{g}_{9/2}\otimes 4_1^+$	$-0.04\ \tilde{g}_{9/2}\otimes 6_1^+$	$-0.02\ \tilde{g}_{9/2}\otimes 6_2^+$
$1/2_2^+$	1.37	4.4	$1.00\ \tilde{g}_{9/2}\otimes 4_2^+$	$+0.10\ \tilde{g}_{9/2}\otimes 4_1^+$	$-0.02\ \tilde{f}_{5/2}\otimes 3_1^-$	$+0.02\ \tilde{g}_{9/2}\otimes 4_3^+$
$3/2_3^+$	1.44	3.9	$1.00\ \tilde{g}_{9/2}\otimes 3_1^+$			

spite of its small energy. Experimentally, this $B(M1)$ value is estimated to $>0.7\mu_N^2$.

The levels which collect the bulk of β-decay intensity are the $1/2^+$ (959 keV) and the two $3/2^+$ states (at 931 and 1015 keV). These levels will be discussed in Sec. V D.

B. Nuclear structure of ^{99}Nb in the MQPM

The even-parity levels, which are those relevant for the allowed transitions, are well reproduced. As in the IBFBPM, in the MQPM the leading components of the $9/2_1^+$, $1/2_1^-$, $7/2_1^+$, $5/2_1^+$, $11/2_1^+$, $9/2_2^+$ and $13/2_1^+$ are the $\pi\tilde{g}_{9/2}$ and $\pi\tilde{p}_{1/2}$ quasiparticle states and the $\pi\tilde{g}_{9/2}\otimes 2_1^+$ multiplet, respectively. The lowest spin members of the multiplet, $7/2_1^+$, $5/2_1^+$, are at the same position as in the IBFBPM but the other members of the multiplet are in a different order (see Fig. 4 and Table VII). In the MQPM calculation the $3/2_1^+$ and $5/2_2^+$ levels belong to the $g_{9/2}\otimes 4_1^+$ multiplet. This configuration was also obtained in the IBFBPM calculation for the 817 keV $5/2^+$ level, but it does not seem that the 765 keV level could be identified with this $3/2^+$ state. The states with strong β-decay feedings are some 400 keV too high in the MQPM. They will be discussed in Sec. V D. Finally, the $3/2_1^-$ and $5/2_1^-$ negative-parity states are predicted to be based on the $p_{1/2}\otimes 2_1^+$ doublet in disagreement with the proton pickup data [37]. This follows from the fact that the $p_{1/2}$ one-quasiparticle state is far too low in energy, leading to an unperturbed energy of the $p_{1/2}\otimes 2_1^+$ doublet, that is too low.

C. Comparison of levels in the $N=58$ isotones ^{97}Y and ^{99}Nb

The singularity of the $d_{5/2}$ subshell closure, which enlarges the level gaps in ^{97}Nb with 56 neutrons, restricts the possibility for a simple extrapolation of levels to ^{99}Nb. Nevertheless, Fig. 5 shows a smooth evolution of the level sequences, since only the closely lying $5/2^+$ and $3/2^-$ levels change their position between ^{97}Nb and ^{99}Nb. The systematics of spherical levels ends at ^{99}Nb since, like their lower-Z neighboring nuclei, Nb isotopes experience the onset of deformation at $N=60$ with ^{101}Nb [7].

Alternatively, comparison of levels of $N=58$ odd-proton nuclei versus a change of proton number by an increment of two is of interest in this particular case. The $N=59$ parent nuclei of ^{99}Nb neighbors have the same spin and parity of $I^\pi=1/2^+$. Consequently, one can expect that their β decay will populate levels of same spins and parities in their respective daughter nuclei ^{97}Y, ^{99}Nb, and ^{101}Tc. A comparison of ^{99}Zr to ^{99}Nb and ^{101}Mo to ^{101}Tc decays is, however, not very meaningful due to the opening of the neutron shell at $Z>40$ [21,37] which changes the nature of the levels in ^{101}Mo [22] and of the onset of deformation in its daughter ^{101}Tc [63]. In contrast, a close correspondance is found between the levels in ^{99}Nb and ^{97}Y shown on the right-hand side of Fig. 5.

The $9/2^+$ and $1/2^-$ single proton quasiparticle levels exchange their positions from ^{97}Y to ^{99}Nb, due to the filling of the $p_{1/2}$ subshell at $Z=40$.

The next ^{97}Y levels at 697 and 954 keV are $3/2^-$ and $5/2^-$ states, where we assume the 697 keV level to be the $5/2^-$ state. This makes ^{97}Y the only nucleus among Y and Nb isotopes with $N>50$ where the $5/2^-$ state is the lowest one. Büscher *et al.* [10] discussed the 954 keV state as being the $5/2^-$ state from the $p_{1/2}\otimes 2^+$ coupling. They based their arguments on the enhancement >6.5 if $E2$ multipolarity for the 954 keV transition is assumed, a value consistent with the rates of the $2^+\rightarrow 0^+$ transitions in the even-even neighbors. Nevertheless, admixtures of single-particle configurations could lead to a smaller collectivity consistent with the value of 2.9 single-particle units if the 697 keV level is the $5/2^-$ level. As a matter of fact, transfer reactions of Flynn *et al.* [37] show the lowest-lying $3/2^-$ (544 keV) and $5/2^-$ (631 keV) levels in ^{99}Nb to be mainly of the $p_{3/2}$ and $f_{5/2}$ hole character. There is no obvious reason why these levels would become more collective in ^{97}Y.

The state at 1320 keV in ^{97}Y has $I^\pi=5/2^+$ [29]. The 652 keV transition to the $9/2^+$ isomer has a rate of 11(4) single-particle units [10]. This value compares well with the 4.8 rate of the 469 keV transition in ^{99}Nb. Therefore, the 1320 keV level in ^{97}Y and the 469 keV level in ^{99}Nb are both built on the $g_{9/2}\otimes 2^+$ configuration. This interpretation was

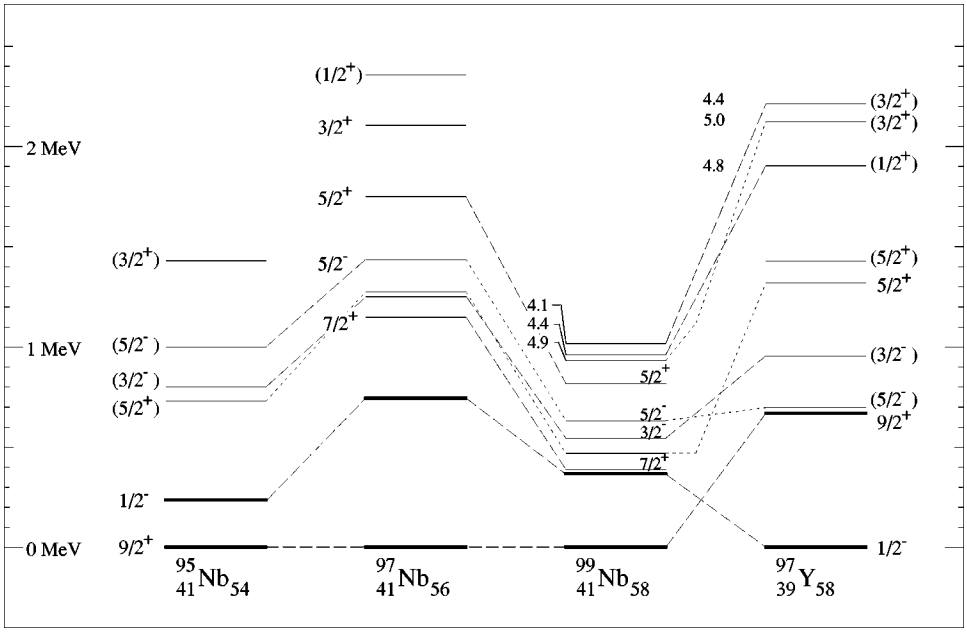

FIG. 5. Systematics of selected low-lying levels in Nb isotopes and in ^{97}Y, the isotone of ^{99}Nb. Dashed and dotted lines connect levels of even and odd parity, respectively. The picture displays similarities of the isotones ^{99}Nb and ^{97}Y in spite of the shell effects being larger in yttrium than in niobium isotopes and of the exchange of the positions of the $\tilde{p}_{1/2}$ and $\tilde{g}_{9/2}$ quasiparticles.

also proposed in Refs. [10,28].

The level at 1428 keV in ^{97}Y was discussed by Büscher *et al.* [10] as the $7/2^+$ level belonging to the $g_{9/2}\otimes 2^+$ coupling, corresponding to the 387 keV level in ^{99}Nb. However, they noticed the unusually small rate of the $E2$ transition (even when assuming no $M1$ component) to the $9/2^+$ single-particle state. According to our new data, this level is a $5/2^+$ state. It seems impossible in the spherical model space to create another $5/2^+$ level so close to the $5/2^+$ state at 1320 keV. Hence, it could be that the 1428 keV level is the head of a band corresponding to a deformed potential minimum. Firstly, the excitation energy for the $5/2^+$ level in ^{97}Y is close to the 1436 keV energy of the deformed 0_3^+ state in ^{98}Zr [15]. Secondly, $I^\pi = 5/2^+$ is the probable spin and parity of the lowest band built on a deformed minimum in ^{97}Y since the [422]5/2 Nilsson orbital is the ground state of the deformed ^{99}Y [64,65], ^{101}Y [66], and ^{103}Y [67] isotopes. Continuing this interpretation, one can find a number of levels, with weak decay branchings to the low-lying levels and energy spacings ressembling those of rotational levels in the heavier Y isotopes. The 3/2 level (of unknown parity) at 1739 keV is indeed a reasonable candidate for the [301]3/2 band head. The 1613 and 1848 keV levels could be very tentatively $5/2^-$ states corresponding to the [303]5/2 band head and the member of the [301]3/2 band, respectively. However, this appealing interpretation of the 1428 keV level seems at variance with the rate >4 (using the half-life upper limit of 8 ps at 3 standard deviations [10]) of the $E2$ transition from the 1905 keV level to the state at 1428 keV, since a hindrance is generally observed for transitions between different shapes. At least, it would be worthwhile to check the above interpretation by searching for a band structure on top of the 1428 keV level. In ^{99}Nb the second $5/2^+$ state is the 817 keV level for which a two-phonon coupled state seems a more probable configuration (see Sec. V A).

Finally, among the highest-lying levels observed in β decay, both in ^{99}Nb and ^{97}Y, there are three levels with very strong direct β feedings which should include a large amplitude of the $\pi g_{9/2}\otimes(\nu g_{7/2}\otimes \nu s_{1/2})_{3,4}$ configuration. This can form one $1/2^+$ and two $3/2^+$ levels in agreement with our proposed assignments. The $I^\pi = 3/2^+$ levels, at 931 keV (^{99}Nb) and at 2121 keV (^{97}Y), present similar decay properties. Both have a weak branch to the $1/2^-$ level (even not observed in ^{99}Nb), but a strong branch to the lowest lying $(g_{9/2}\otimes 2^+)_{5/2^+}$ level. The other $I^\pi = 3/2^+$ levels, at 1015 keV in ^{99}Nb and 2212 keV in ^{97}Y, have a similar decay pattern, since they decay to almost all levels which can be reached via dipole or electric quadrupole transitions, and also have the lowest logft values (4.4 and 4.1, respectively). On the basis of analogy we have proposed the $I^\pi = 1/2^+$ assignment for the 1905 keV level in ^{97}Y, corresponding to the 959 keV level in ^{99}Nb. For both $E2$ transitions to the $(g_{9/2}\otimes 2^+)_{5/2^+}$ levels a rate larger than 1.2 s.p. units (using the three σ limit for ^{97}Y) is deduced. The branching to the possibly deformed 1428 keV level in ^{97}Y has no counterpart in ^{99}Nb, probably due to the lower energy of the $1/2^+$ level in the latter nucleus. With the new $3/2^-$ assignment of the 954 keV level in ^{97}Y the ratio $B(E1,1/2^+\rightarrow 3/2^-)/B(E1,1/2^+\rightarrow 1/2^-)$ is equal to 0.52 for ^{99}Nb and 0.66 for ^{97}Y. These values are close to each other. As a conclusion of this comparison it turns out that β feedings and γ-decay rates of corresponding levels in ^{97}Y and ^{99}Nb are very similar.

D. β-decay properties

The $N=59$ isotones ^{97}Sr and ^{99}Zr have the $1/2^+$ ground state associated with the $s_{1/2}$ neutron. The two other valence neutrons (outside of the $d_{5/2}$ subshell) mainly occupy the $g_{7/2}$ orbital. Thus, β decays of Sr and Zr parents can be explained by the Gamow-Teller transition of one of the $g_{7/2}$ paired

neutrons, leading to the $\pi\tilde{g}_{9/2}\otimes(\nu\tilde{g}_{7/2}\otimes\nu\tilde{s}_{1/2})_{3,4}$ configuration in daughter nuclei, resulting in three strongly fed states ($I^\pi=1/2^+$, $3/2^+$, $3/2^+$). The $N=57$ isotones ^{95}Sr [19] and ^{97}Zr [20] also have a $1/2^+$ ground state. In the absence of a strong $N=56$ neutron shell closure, the occupation probability of the $g_{7/2}$ neutron orbital should vary smoothly versus neutron number and the β-decay pattern of the $N=57$ and $N=59$ isotones should be quite similar, except for some slowing down of the transitions for $N=57$. In contrast, experiments show dramatic differences. In the decays of the $N=57$ isotones ^{95}Sr and ^{97}Zr, allowed transitions are slower by at least one order of magnitude [34]. In the decay of ^{95}Sr to ^{95}Y, the lowest logft values are 6.1 and 5.7 for two levels at 2717 and 2933 keV, respectively, and in the decay of ^{97}Zr to ^{97}Nb the lowest logft value is 6.5 for the 2106 keV level. As a matter of fact, the strongest β branchings in terms of intensity are due to first-forbidden decays of the $\nu s_{1/2}\rightarrow\pi p_{1/2}$ type. The reduction of allowed transition rates suggests a dramatic reduction of the occupation of the $g_{7/2}$ neutron pair, which can be regarded as a further evidence for the shell gap at $N=56$.

In the IBFM wave functions of the $1/2^+$ ground states of ^{99}Zr and ^{97}Sr, the dominant component is the $\nu\tilde{s}_{1/2}$ quasineutron state [9,17,61], while in the IBFBPM wave functions of the $1/2^+$ and $3/2^+$ states around 1 MeV of excitation energy in ^{99}Nb the largest components are the $|\pi\tilde{g}_{9/2},24;1/2\rangle$, $|\pi\tilde{g}_{9/2},24;3/2\rangle$, $|\pi\tilde{g}_{9/2},33;3/2\rangle$, $|\pi\tilde{g}_{9/2},44;1/2\rangle$, $|\pi\tilde{g}_{9/2},44;3/2\rangle$, i.e., the two-, three-, and four-d-boson components, respectively. As shown in Ref. [9], there are sizeable admixtures of the $|\nu\tilde{g}_{7/2},24;1/2\rangle$ component in the ground states of ^{99}Zr and ^{97}Sr. This component leads to the population of the main components in the $1/2^+$ and $3/2^+$ states in ^{99}Nb and ^{97}Y by Gamow-Teller decay of the $\tilde{g}_{7/2}$ neutron to the $\tilde{g}_{9/2}$ proton. The other sizeable admixture in the wave function of parent nuclei is the $|\nu\tilde{d}_{3/2},12;1/2\rangle$ component, which leads in β decay to the population of the $|\pi\tilde{d}_{5/2},12;1/2\rangle$ and $|\pi\tilde{d}_{5/2},12;3/2\rangle$ admixtures in the wave functions of daughter nuclei.

Another contribution arises when one s boson in the main component $|\nu\tilde{s}_{1/2},00;1/2\rangle$ of the $1/2^+$ parent state undergoes a Gamow-Teller decay, in which the $(\nu\tilde{g}_{7/2})^2_0$ pair in the internal structure of the s boson is transformed into the $(\pi\tilde{g}_{9/2}\nu\tilde{g}_{7/2})_1$ configuration. This leads to the population of $\pi\tilde{g}_{9/2}\nu\tilde{g}_{7/2}\nu\tilde{s}_{1/2}$ three-quasiparticle configurations in the intrinsic structure of the $1/2^+$ and $3/2^+$ states of daughter nuclei. In other words, the β decay of ^{99}Zr populates the $(\nu\tilde{g}_{7/2},\nu\tilde{s}_{1/2})3$ and $(\nu\tilde{g}_{7/2},\nu\tilde{s}_{1/2})4$ components of the internal structure of boson states contained in the IBFBPM wave functions of $1/2^+$ and $3/2^+$ states of ^{99}Nb.

In the MQPM, for the core nucleus all the relevant states, 4^+_1, 3^+_1 and 4^+_2, have large $\nu\tilde{g}_{7/2}\nu\tilde{s}_{1/2}$ components in their internal structure (Table VIII). There are five $1/2^+$ and $3/2^+$ states based on these core states coupled to the $\pi\tilde{g}_{9/2}$ quasiproton, namely the two $1/2^+$ ($\pi\tilde{g}_{9/2}\otimes4^+_1$, $\pi\tilde{g}_{9/2}\otimes4^+_2$) and three $3/2^+$ states ($\pi\tilde{g}_{9/2}\otimes4^+_1$, $\pi\tilde{g}_{9/2}\otimes4^+_2$, $\pi\tilde{g}_{9/2}\otimes3^+_1$). All these five states have large $\pi\tilde{g}_{9/2}\nu\tilde{g}_{7/2}\nu\tilde{s}_{1/2}$ components and are predicted to be sizably populated in β decay of the $1/2^+$ ground state of ^{99}Zr. Additional small contributions to the β decay arise due to small admixtures to the dominant $\nu\tilde{s}_{1/2}\otimes0^+_1$ component in the MQPM wave function of the $1/2^+$ ground state of ^{99}Zr: $0.177\nu\tilde{d}_{5/2}\otimes2^+_1$ and $-0.52\nu\tilde{g}_{7/2}\otimes4^+_1$.

TABLE VIII. Two-quasineutron internal structure of the 4^+_1, 3^+_1, and 4^+_2 states of the reference nucleus ^{98}Zr calculated in the MQPM.

	4^+_1 0.92 MeV	3^+_1 1.32 MeV	4^+_2 1.25 MeV
$\nu\tilde{g}_{7/2}\nu\tilde{s}_{1/2}$	−0.63	−0.99	0.74
$\nu\tilde{g}_{7/2}\nu\tilde{d}_{3/2}$	0.24	−0.02	0.01
$\nu\tilde{g}_{7/2}\nu\tilde{d}_{5/2}$	0.18	−0.01	0.04
$\nu\tilde{g}_{7/2}\nu\tilde{g}_{7/2}$	−0.64	0	−0.66
$\nu\tilde{d}_{5/2}\nu\tilde{d}_{3/2}$	0.23	−0.02	0.06
$\nu\tilde{d}_{5/2}\nu\tilde{s}_{1/2}$	0	0.05	0

We note that the 4^+_1 state of the MQPM corresponds to the $n_d=2$ state of the IBFBPM, and 3^+_1, 4^+_2 states of the MQPM to the $n_d=3$ states. In this sense we find a qualitative analogy between the MQPM and IBFBPM calculations, only the mixing of the $n_d=2$ and $n_d=3$ IBM boson states is stronger for the IBFBPM. However, in both calculations we encounter the same problem: all three calculated low-lying $3/2^+$ states are sizeably populated in β decay, while experimentally one of these states (the lowest one at 765 keV) is weakly populated. A similar problem appears for one of the two $1/2^+$ states.

Concluding, the calculations provide five $1/2^+$, $3/2^+$ states having sizable $\pi\tilde{g}_{9/2}\nu\tilde{g}_{7/2}\nu\tilde{s}_{1/2}$ components in their internal structure, arising from five basis states, leading to sizable population in β decay. Since there is no way to reduce the number of relevant basis states from five to three, we conclude that an additional mixing in the wave functions is needed in order to produce destructive interference among the contributions from the $n_d=2$ and $n_d=3$ components to β-decay matrix elements in one $3/2^+$ and one $1/2^+$ state of ^{99}Nb. In the present calculation we have not succeeded in simulating such a destructive interference.

VI. SEARCH FOR A HIGH-SPIN ISOMER IN ^{99}Nb

Several experimental [24] and theoretical works [25,26] have been devoted to levels in ^{97}Y populated by the $E3$ isomeric decay of its $(\pi\tilde{g}_{9/2}\otimes\nu\tilde{g}_{7/2}\otimes\nu\tilde{h}_{11/2})_{27/2^-}$ three-quasiparticle isomer. Especially interesting is the rare opportunity to observe high-spin states generated by a $g_{9/2}$ proton coupled to core excitations or a broken neutron pair. In these states the odd proton has been lifted from the $p_{1/2}$ to the $g_{9/2}$ shell, leaving the $p_{1/2}$ orbital empty. Similar states could be formed in ^{99}Nb by simply filling the $p_{1/2}$ shell with the two extra protons paired to $I^\pi=0^+$. Experimental evidence for a three-quasiparticle isomer in ^{99}Nb was first searched via its β decay to the known yrast levels in ^{99}Mo [21]. This experiment was not successful but did not yet exclude the possibility of the alternative isomeric decay branching to levels in ^{99}Nb.

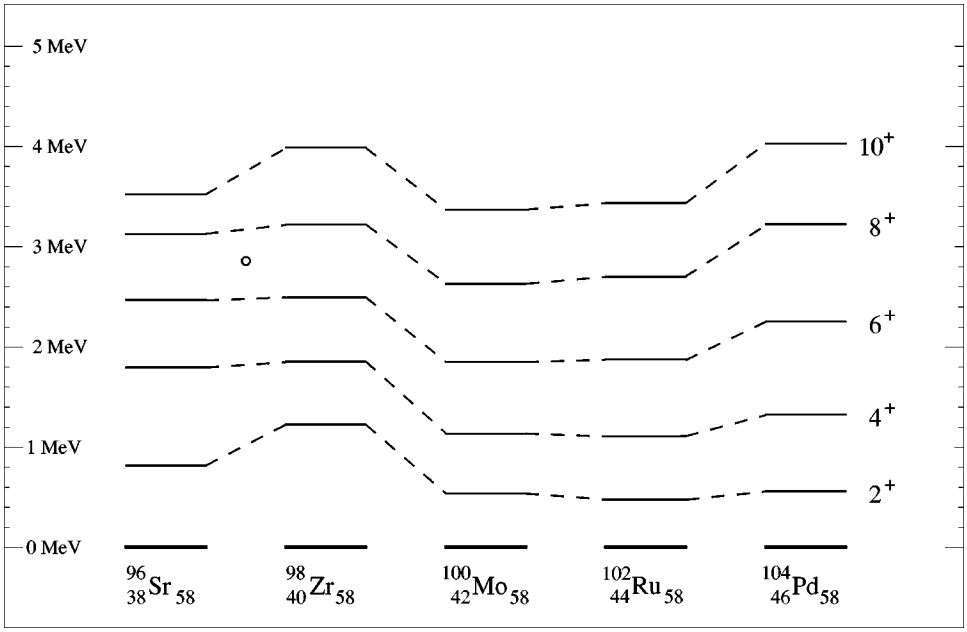

FIG. 6. Yrast levels in the $N=58$ neighboring isotones of ^{99}Nb. The distance between the $(\tilde{g}_{7/2}\otimes\tilde{h}_{11/2})_{9^-}$ broken neutron pair (the estimate for ^{97}Y is shown by an open circle) and the 6^+ yrast level is crucial for the existence of an isomer.

Fingerprints of such a decay are the presence of a strongly converted transition, which can be assigned by the characteristic Nb K-x rays, followed by a cascade of γ rays of comparable intensities and whose energies remind of the spacings between the yrast levels of the even-even core. A sequence of γ rays with these characteristics was searched in the γ-γ and x-γ matrices. In addition, matrices of three- and four-fold events were analyzed, since higher coincidence folds should emphasize the γ rays belonging to cascades of large multiplicity. However, no evidence for the searched patterns was found. Assuming, by analogy with the ^{97}Y data [20], that the independent population of the high-spin isomer is approximately 3% of the total independent Nb population, then about 70 ions must be transported per second to the collection spot. The limit for the detection of a cascade of 500 keV γ rays in this experiment is estimated to 7 ions/sec. Hence, we must conclude that the postulated high-spin configuration in ^{99}Nb is not an isomer, the half-life of which is long enough to survive the time ($\simeq$1 ms) between its production and the measurement.

The isomeric $E3$ transition corresponds to a neutron transition in which the 9^- broken pair changes to 6^+. The energies of $(\tilde{g}_{7/2}\otimes\tilde{h}_{11/2})_{9^-}$ broken neutron pairs in the neighboring even-even isotopes are unknown. A crude estimate can be obtained from ^{97}Y by subtracting the experimental $\pi g_{9/2}$ energy of 668 keV from the energy of 3523 keV of the $(\pi\tilde{g}_{9/2}\otimes\nu\tilde{g}_{7/2}\otimes\nu\tilde{h}_{11/2})_{27/2^-}$ configuration. Figure 6 shows the yrast levels in $N=58$ isotones [11,34]. The estimated 9^- broken pair energy is well below the yrast 8^+ levels in both neighboring core nuclei, and the only possible electromagnetic decay is the $E3$ transition to the yrast 6^+ level. The experimental $E_\gamma(27/2^-\rightarrow 21/2^+)$ energy of 162 keV is even a bit lower than the unperturbed 9^- to 6^+ energy difference of 376 keV (taking the average 6^+ state energies in ^{96}Sr and ^{98}Zr), probably due to the coupling of these core states with the $g_{9/2}$ proton. The even-even neighbors for ^{99}Nb are ^{98}Zr and ^{100}Mo. From the discussion of level structure the latter seems a more appropriate core in which the yrast levels become lower. Thus, with the same assumptions as above, the 9^- to 6^+ energy gap increases and the experimental $E_\gamma(27/2^-\rightarrow 21/2^+)$ transition energy should be about 470 keV. For an $E3$ transition with the same rate characteristics as the one in ^{97}Y, the estimated lifetime of 0.17 ms is indeed too short to allow observation of the isomer after mass separation. In the present calculation we obtain the $27/2^-$ three-quasiparticle configuration at 2.72 MeV above the $\pi\tilde{g}_{9/2}$ ^{99}Nb ground state. This is in accordance with the conclusion of the too high energy of the $E3$ transition to the $[\pi\tilde{g}_{9/2}\otimes 6^+]21/2^+$ level being responsible for the nonobservation of the $27/2^-$ level.

The ultimate condition for isomerism is that the 9^- level should be below the yrast 8^+ level in order to prevent its $E1$ decay. This gives a maximum energy of 753 keV for the $E3$ transition, which translates into a half-life of 6 μs. Therefore, there still should be a fair chance to observe the $27/2^-$ three-quasiparticle configuration in ^{99}Nb at a recoil separator.

VII. CONCLUSION

The decay schemes of ^{99}Zr to ^{99}Nb and of ^{97}Sr to ^{97}Y have been reinvestigated. The former now includes several transitions with absolute decay branchings lower than 10^{-3}. A few additional transitions have been found in the latter that allow a new interpretation of some levels. Several level spin and parity assignments have been revised; $I^\pi=3/2^+$ for the 931 keV level in ^{99}Nb and $I^\pi=5/2^+$ for the 1428 keV level in ^{97}Y. The levels at 959 keV in ^{99}Nb and 1905 keV in ^{97}Y are proposed to be $1/2^+$ states. This requires the 697 and 954 keV levels in ^{97}Y to be the $5/2^-$ and $3/2^-$ states, respectively, at variance with previously made assignments. In spite of the compression of level energies in ^{99}Nb with re-

spect to ^{97}Y, several levels of the same character are observed. The $5/2^+$ levels at 1320 keV in ^{97}Y and 469 keV in ^{99}Nb are both built on the $g_{9/2}\otimes 2^+$ configuration. New similarities emerge for three strongly populated levels, two firmly assigned $3/2^+$ states and a probable $1/2^+$ level, which have comparable log*ft* values and decay rates in both nuclei. This indicates that the $N=56$ shell closure is still active for ^{99}Nb, in contrast to its vanishing with only two extra protons giving a deformed character to ^{101}Tc.

The observation of high-spin states in ^{99}Nb has so far been impossible due to the lack of evidence for a three-particle $27/2^-$ state in decay experiments. The too short level lifetime is interpreted as a consequence of the increase of the softness of the ^{100}Mo core with respect to the ^{96}Sr and ^{98}Zr neighbors.

Finally, it is tempting to assign the $I^\pi=5/2^+$ 1428 keV level in ^{97}Y as the [422]5/2 head of a deformed band. Confirmation of this assumption would put the picture of shape coexistence in the $N=58$–60 region on a firmer ground. Prompt fission should be the best technique for searching whether any band structure is built on this level.

ACKNOWLEDGMENTS

The authors wish to thank the K-130 cyclotron group for the steady improvements in beam intensity and K. Loberg and M. Lahtinen for development of the VENLA acquisition system. This work was financially supported by the Academy of Finland and of the European Community via the Human Capital and Mobility and Training and Mobility of Researchers programs.

[1] See, for instance, contributions by G. Molnár *et al.*, T. Belgya *et al.*, E.A. Henry *et al.*, and M.L. Stolzenwald *et al.*, in *Proceedings of International Workshop on Nuclear Structure of the Zr Region*, Bad Honnef, Germany, 1988, edited by J. Eberth, R.A. Meyer, and K. Sistemich (Springer-Verlag, Berlin, 1988).

[2] E. Cheifetz, R.C. Jared, S.G. Thompson, and J.B. Wilhelmy, Phys. Rev. Lett. **25**, 38 (1970).

[3] H. Ohm, G. Lhersonneau, K. Sistemich, B. Pfeiffer, and K.-L. Kratz, Z. Phys. A **327**, 483 (1987).

[4] H. Mach, F.K. Wohn, M. Moshzynski, R.L. Gill, and R.F. Casten, Phys. Rev. C **41**, 1141 (1990).

[5] H. Ohm, M. Liang, G. Molnär, and K. Sistemich, Z. Phys. A **334**, 519 (1989).

[6] H. Mach, M. Moszynski, R.L. Gill, F.K. Wohn, J.A. Winger, J.C. Hill, G. Molnár, and K. Sistemich, Phys. Lett. B **230**, 21 (1989).

[7] H. Ohm, M. Liang, U. Paffrath, B. De Sutter, K. Sistemich, A.-M. Schmitt, N. Kaffrell, N. Trautmann, T. Seo, K. Shizuma, G. Molnár, K. Kawade, and R.A. Meyer, Z. Phys. A **340**, 5 (1991).

[8] M. Liang, H. Ohm, B. De Sutter, K. Sistemich, B. Fazekas, and G. Molnár, Z. Phys. A **340**, 223 (1991).

[9] G. Lhersonneau, B. Pfeiffer, K.-L. Kratz, H. Ohm, K. Sistemich, S. Brant, and V. Paar, Z. Phys. A **337**, 149 (1990).

[10] M. Büscher, R.F. Casten, R.L. Gill, R. Schuhmann, J.A. Winger, H. Mach, M. Moszynski, and K. Sistemich, Phys. Rev. C **41**, 1115 (1990).

[11] J.H. Hamilton, A.V. Ramayya, S.J. Zhu, G.M. Ter-Akopian, Yu. Oganessian, J.D. Cole, J.O. Rasmussen, and M.A. Stoyer, Prog. Part. Nucl. Phys. **36**, 635 (1995).

[12] H. Mach and R.L. Gill, Phys. Rev. C **36**, 2721 (1987).

[13] S. Brant, V. Paar, G. Lherssoneau, O.W.B. Schult, H. Seyfahrt, and K. Sistemich, Z. Phys. A **334**, 517 (1989).

[14] G. Lhersonneau, R.A. Meyer, K. Sistemich, H.P. Kohl, H. Lawin, G. Menzen, H. Ohm, T. Seo, and D. Weiler, *Proceedings of the American Chemical Society Symposium on Nuclei off the Line of Stability*, edited by R.A. Meyer and D.S. Brenner (American Chemical Society, Chicago, 1986), Vol. 324, p. 202.

[15] G. Lhersonneau, B. Pfeiffer, K.-L. Kratz, T. Enqvist, P.P. Jauho, A. Jokinen, J. Kantele, M. Leino, J.M. Parmonen, H. Penttilä, J. Äystö, and the ISOLDE Collaboration, Phys. Rev. C **49**, 1379 (1994).

[16] G. Lhersonneau, P. Dendooven, A. Honkanen, M. Huhta, P.M. Jones, R. Julin, S. Juutinen, M. Oinonen, H. Penttilä, J.R. Persson, K. Peräjärvi, A. Savelius, J.C. Wang, and J. Äystö, Phys. Rev. C **56**, 2445 (1997).

[17] S. Brant, V. Paar, and A. Wolf, *Proceedings of 9th International Symposium on Capture Gamma-Ray Spectroscopy and Related Topics*, Budapest, Hungary, 1996, edited by G. Molnár and T. Belgya (Springer, Budapest, 1997), Vol. 1, p. 276.

[18] W. Urban, J.L. Durell, W.R. Phillips, A.G. Smith, M.A. Jones, I. Ahmad, A.R. Barnett, M. Bentaleb, S.J. Dorning, M.J. Leddy, E. Lubkiewicz, L.R. Moore, T. Rzaca-Urban, R.A. Sareen, N. Schulz, and B.J. Varley, Z. Phys. A **358**, 145 (1997).

[19] K.-L. Kratz, H. Ohm, A. Schroder, H. Gabelmann, W. Ziegert, B. Pfeiffer, G. Jung, E. Monnand, J.A. Pinston, R. Schussler, G.I. Crawford, S.G. Prussin, and Z.M. de Oliveira, Z. Phys. A **312**, 43 (1983).

[20] G. Lhersonneau, P. Dendooven, S. Hankonen, A. Honkanen, M. Huhta, R. Julin, S. Juutinen, M. Oinonen, H. Penttilä, A. Savelius, S. Törmänen, J. Äystö, P.A. Butler, J.F.C. Cocks, P.M. Jones, and J.F. Smith, Phys. Rev. C **54**, 1117 (1996).

[21] G. Lhersonneau, B. Pfeiffer, J.R. Persson, J. Suhonen, J. Toivanen, P. Campbell, P. Dendooven, A. Honkanen, M. Huhta, P.M. Jones, R. Julin, S. Juutinen, M. Oinonen, H. Penttilä, A. Savelius, J.C. Wang, and J. Äystö, Z. Phys. A **358**, 317 (1997).

[22] H. Seyfarth, H.H. Guven, B. Kardon, G. Lhersonneau, K. Sistemich, S. Brant, N. Kaffrell, P. Maier-Komor, H.K. Vonach, V. Paar, D. Vorkapic, and R.A. Meyer, Z. Phys. A **339**, 269 (1991).

[23] H. Mach, F.K. Wohn, G. Molnár, K. Sistemich, J.C. Hill, M. Moszynski, R.L. Gill, W. Krips, and D.S. Brenner, Nucl. Phys. **A523**, 197 (1991).

[24] G. Lhersonneau, P. Butler, J.F.C. Cocks, A. Honkanen, M. Huhta, P.M. Jones, A. Jokinen, R. Julin, S. Juutinen, A. Lampinen, D. Müller, E. Mäkelä, M. Oinonen, J.M. Parmonen, P. Piiparinen, A. Savelius, J.F. Smith, S. Törmänen, A. Virtanen,

and J. Äystö, Nucl. Instrum. Methods Phys. Res. A **373**, 415 (1996).
[25] S. Brant, K. Sistemich, V. Paar, and G. Lhersonneau, Z. Phys. A **330**, 365 (1988).
[26] G. Lhersonneau, S. Brant, V. Paar, and D. Vretenar, Phys. Rev. C **57**, 681 (1998).
[27] B. Pfeiffer, E. Monnand, J.A. Pinston, F. Schussler, C. Jung, J. Münzel, and H. Wollnik, in *Proceedings of the International Conference on Nuclei far from Stability*, Helsingor, Denmark, Vol. 2, CERN 81-89 (1981), p. 423.
[28] H. Ohm, KFA-Jülich Annual Report, Jul-Spez-562, p. 34 (90).
[29] L.K. Peker, Nucl. Data Sheets **73**, 1 (1994).
[30] B. Pfeiffer, E. Monnand, J.A. Pinston, H. Lawin, and J. Münzel, Annual Report ILL 3-06-22 (1984).
[31] P. Taskinen, H. Penttilä, J. Äystö, P. Dendooven, P. Jauho, A. Jokinen, and M. Yoshi, Nucl. Instrum. Methods Phys. Res. A **281**, 539 (1989).
[32] M. Huhta, P. Dendooven, A. Honkanen, G. Lhersonneau, M. Oinonen, H. Penttilä, K. Peräjärvi, V. Rubchenya, and J. Äystö, *Proceedings of the EMIS-13 Conference*, Bad Dürkheim, 1996, Germany [Nucl. Instrum. Methods Phys. Res. B **126**, 201 (1997)].
[33] H. Penttilä, P. Dendooven, A. Honkanen, M. Huhta, G. Lhersonneau, M. Oinonen, J.M. Parmonen, K. Peräjärvi, and J. Äystö, *Proceedings of the EMIS-13 Conference* (Ref. [32]), p. 213.
[34] R.B. Firestone, *Table of Isotopes*, 8th ed. (Wiley, New York, 1996).
[35] J. McPherson, IEEE Trans. Nucl. Sci. **39**, 806 (1992).
[36] K. Jääskeläinen, P.M. Jones, A. Lampinen, K. Loberg, and W. Trzaska, JYFL Annual Report 1995, p. 15 (1996).
[37] E.R. Flynn, R.E. Brown, F. Ajzenberg-Selove, and J.A. Cizewski, Phys. Rev. C **28**, 575 (1983).
[38] J. Kantele, computer program, in *Handbook of Nuclear Spectrometry* (Academic, San Diego, 1995), ISBN 0-12-396440-7.
[39] G. Battistuzzi, K. Kawade, H. Lawin, K. Shizuma, and K. Sistemich, Z. Phys. A **306**, 113 (1982).
[40] H.A. Selič, G. Sadler, T.A. Khan, W.D. Lauppe, H. Lawin, K. Sistemich, E. Monnand, J. Blachot, J.P. Bocquet, and F. Schussler, Z. Phys. A **289**, 197 (1979).
[41] P.K. Bindal, D.H. Youngblood, and R.L. Kozub, Phys. Rev. C **10**, 729 (1974).
[42] A. Arima and F. Iachello, Phys. Rev. Lett. **35**, 1069 (1975).
[43] F. Iachello and A. Arima, *The Interacting Boson Model* (Cambridge University Press, Cambridge, 1987).
[44] A. Arima and F. Iachello, Ann. Phys. (N.Y.) **99**, 233 (1976); **111**, 201 (1978); **123**, 468 (1979).
[45] D. Janssen, R.V. Jolos, and F. Dönau, Nucl. Phys. **A224**, 9 (1974).
[46] V. Paar, in *Interacting Bosons in Nuclear Physics*, edited by F. Iachello (Plenum, New York, 1979), p. 163.
[47] F. Iachello and O. Scholten, Phys. Rev. Lett. **43**, 679 (1979).
[48] F. Iachello and P. Van Isacker, *The Interacting Boson Fermion Model* (Cambridge University Press, Cambridge, 1991).
[49] V. Paar, S. Brant, L.F. Canto, G. Leander, and M. Vouk, Nucl. Phys. **A378**, 41 (1982).
[50] V. Paar, *Proceedings of the International Symposium on Inbeam Nuclear Spectroscopy*, edited by Zs. Dombrádi and T. Fényes (Akademiai Kiado, Budapest, 1984), Vol. 2, p. 675; *Proceedings of the International Symposium on Capture Gamma-ray Spectroscopy and Related Topics*, edited by S. Raman, AIP Conf. Proc. No. **125** (AIP, New York, 1984), p. 70.
[51] S. Brant, V. Paar, and D. Vretenar, Z. Phys. A **319**, 355 (1984); S. Brant and V. Paar, *ibid.* **329**, 151 (1988).
[52] F. Iachello and D. Vretenar, Phys. Rev. C **43**, 945 (1991).
[53] D. Vretenar, V. Paar, G. Bonsignori, and M. Savoia, Phys. Rev. C **42**, 993 (1990); **44**, 223 (1991).
[54] C.J. Lister, P. Chowdhury, and D. Vretenar, Nucl. Phys. **A557**, 361c (1993).
[55] D. Vretenar, G. Bonsignori, and M. Savoia, Z. Phys. A **351**, 289 (1995).
[56] J. Toivanen and J. Suhonen, J. Phys. G **21**, 1491 (1995); Phys. Rev. C **57**, 1237 (1998).
[57] J. Suhonen, J. Toivanen, A. Holt, T. Engeland, E. Osnes, and M. Hjorth-Jensen, Nucl. Phys. **A628**, 41 (1998).
[58] A. Bohr and B.R. Mottelson, *Nuclear structure, Vol I* (Benjamin, New York, 1969).
[59] J. Suhonen, T. Taigel, and A. Faessler, Nucl. Phys. **A486**, 91 (1988).
[60] J. Suhonen, Nucl. Phys. **A563**, 205 (1993).
[61] S. Brant, V. Paar, and A. Wolf (unpublished).
[62] T. Fényes, A. Algora, Zs. Podolyák, D. Sohler, J. Timär, S. Brant, V. Paar, and Lj. Šimičić, Phys. Part. Nuclei **26**, 831 (1995).
[63] D.G. Savage, H. Aslan, B. Crowe, T. Dague, S. Zeghib, F.A. Rickey, and P.C. Simms, Phys. Rev. C **55**, 120 (1997).
[64] R.A. Meyer, E. Monnand, J.A. Pinston, F. Schussler, I. Ragnarsson, B. Pfeiffer, H. Lawin, G. Lhersonneau, T. Seo, and K. Sistemich, Nucl. Phys. **A439**, 510 (1985).
[65] R.F. Petry, H. Dejbakhsh, J.C. Hill, F.K. Wohn, M. Schmid, and R.L. Gill, Phys. Rev. C **31**, 621 (1985).
[66] R.F. Petry, J.D. Goulden, F.K. Wohn, J.C. Hill, R.L. Gill, and A. Piotrowski, Phys. Rev. C **37**, 2704 (1988).
[67] G. Lhersonneau, P. Dendooven, A. Honkanen, M. Huhta, M. Oinonen, H. Penttilä, J. Äystö, J. Kurpeta, J.R. Persson, and A. Popov, Phys. Rev. C **54**, 1592 (1996).